The shear buckling and postbuckling behavior of laterally pressured curved panels

M.M. Alinia
Dept. of Civil and Environmental Engineering
Amirkabir University of Technology
Tehran 15875-4413, Iran
m.alinia@aut.ac.ir

Arash Saeidpour[1]
School of Environmental, Civil, Agricultural and Mechanical Engineering
University of Georgia
Athens, GA 30602
arashs@uga.edu

Mozhdeh Amani
Dept. of Civil and Environmental Engineering
Amirkabir University of Technology
Tehran 15875-4413, Iran
mozhdehamani@aut.ac.ir

ABSTRACT

Curved panels are widely used in different structures from fuselage of planes to curved bridge girders. An accurate understanding of buckling and postbuckling behavior of curved panels under different loadings is essential for efficient structural design. The shear buckling and postbuckling behavior of laterally pressured thin curved panels under gradually increasing in – plane shear forces is investigated. The magnitude of the lateral forces, the radius of curvature and the aspect ratio of panels are considered in the parametric studies. A classic theoretical formulation of curved panels buckling load is reexamined and compared to experimental results. The results showed that inward pressure eliminates the snap – through phenomenon and the softening stage in the response of shallow curved panels. However, the buckling characteristics are not significantly affected in the moderately curved panels under small pressures. In addition, the magnitude of inward pressures that would affect the shear buckling and postbuckling behavior of panels depends on their radius of curvature. The ultimate shear capacity of a highly curved panel is considerably reduced due to the increasing presence of inward pressures. The failure mode of

[1] Corresponding author

highly curved panels are associated with the occurrence of unstable buckling; and as a result, the released strain energy prevents the occurrence of hardening stages.

1. INTRODUCTION

Curved panels are widely utilized as load–bearing elements in various naval, aerospace and civil engineering structures. Examples of such structures are web plates of curved I – girders, wings and fuselage of planes, ships and boats, missiles, water storage tanks and pressure vessels. These elements are of great interest, where light weight and high in–plane load–bearing capacity is required. In addition to the aforementioned properties, the reserved postbuckling strength of these elements opens extra possibilities for the engineering design. This paper aims to investigate the buckling and postbuckling behavior of curved panels under the combined action of in–plane shear force and lateral normal pressure, commonly found in the above mentioned structures.

There have been some previous researches on the stability of curved panels under pure in–plane shear forces as discussed by Amani et al. [1]. The early works on the theoretical aspects were conducted by Donnell [2]. In a majority of the theoretical treatments of the buckling of cylindrical shells, three simultaneous partial differential equations were used to express the relationship between the components of the shell's median–surface axial, circumferential and radial displacements [3]. Leggett proposed a new set of equations to predict the critical shear stress of a long, slightly bowed sheet [4]. The panels were assumed to be sufficiently long, allowing the short edge boundary conditions to be neglected. The problem with the Donnell's equation is that it only includes the out– of – plane displacements, whereas the boundary conditions on the radial and circumferential boundaries cannot be imposed directly.

Batdorf proposed a method to find the critical shear stress of curved panels by the use of the Donnell's equation [5]. The method presumes that the radial and circumferential boundaries are simply supported. Some curves were computed for the panels under pure shear loading and the results were compared to those obtained by Leggett. Domb presented a

nonlinear modeling technique to predict the buckling of simply supported curved panels under the combined action of shear and compression loads [6]. A set of interaction buckling curves was generated to include the effects of initial imperfections on the combined buckling characteristics.

In general, the buckling and postbuckling behavior of an ideal curved panel under pure in–plane shear force can be divided into the following stages:

a. Linear growth of the in–plane shear force up to the critical shear load,

b. Snap reduction of the shear force immediately after buckling,

c. Further growth of the shear force after reaching a local minimum limit,

d. Reaching the maximum load – bearing capacity,

e. Reduction of the shear force due to the material's softening.

The effect of normal lateral pressure on the buckling behavior of curved panels was further considered during the World War II. The researchers at the National Advisory Committee for Aeronautics (NACA) found that on an airplane in level flight, the upper surface of the wing is subjected to an outward–acting pressure due to the difference in the internal and external pressures [7]. The effect of normal pressure on the stability of thin – walled circular cylinders under torsion was investigated experimentally and theoretically by Rafel and Sandlin [8]. They found that the critical shear stress was appreciably raised by the outward pressure. A semi–empirical interaction formula was derived to predict the critical shear stress. The results of the formula were in good accordance with the experimental results. However, the postbuckling behavior of panels was not considered in that study.

Hopkins and Brown theoretically investigated the stability of long and bowed curved panels under the combined action of normal pressure and shear forces [9]. Their results were in good accordance with the NACA's experimental results. They also considered the influence of boundary conditions on the critical shear stress of the panels and concluded that the difference between the buckling stress of simply supported and clamped edges decreases

rapidly with the curvature and pressure, thus making the indeterminacy of practical edge conditions less important.

Aghajari et al. numerically and experimentally investigated the buckling and postbuckling behavior of thin – walled cylindrical steel shells with varying thickness subjected to uniform external pressure [10]. The results showed that when there is a low variation in the wall thickness, the buckling mode expands over the whole length of the panel; while when there is a high variation in the wall thickness, only the thinner parts are involved. Golzan and Showkati conducted experimental and FE studies to investigate the elastic and plastic responses and asymmetric imperfection sensitivity of truncated conical shells and shallow conical caps under the action of external uniform pressure [11]. Chen et al. described a new method of determining the critical buckling resistance of cylindrical shells with stepped walls exposed to uniform external pressure, and demonstrated the manner in which the method can be used to assess the buckling behavior in a wide range pattern of the wall thickness changes [12].

The buckling and postbuckling behavior of structural elements often involves material and geometric nonlinearities. In slender elements, the load–displacement path shows a limit point, where the curve becomes horizontal or vertical, followed by a snap – through or snap – back. General static analysis procedures like the standard load – control and displacement – control methods encounter problems in snap – through and snap – back points, respectively. The Riks method [13, 14] or the dynamic approaches should be applied to deal with such problems. Kobayashi et al. [15] used a validated static stabilizing method to simulate the successive path – jumping in the deep postbuckling behavioral region of the cylindrical shells under axial compression.

In this paper, the Donnell's equation of equilibrium for curved panels under combined action of normal pressure and shear force was solved by use of the Mathematica software. The calculated critical shear stress coefficients were compared against the NACA's

experimental results. Next, the shear buckling and postbuckling behavior of the perfect curved panels with various curvatures subjected to pure shear forces were investigated via four nonlinear FE analysis methods (i.e., the general static, the arc length, the dynamic explicit, and the dynamic implicit). Results of these analyses were then compared and their advantages and shortcomings were discussed. Subsequently, a set of parametric studies on the laterally pressured curved panels with various curvatures and aspect ratios under gradually increasing in–plane shear was conducted. Both inward and outward pressures were included in these investigations, and the results are presented and discussed.

2. CRITICAL SHEAR STRESS OF PRESSURED CURVED PANELS

In this section, the modified form of the Donnell's equation of equilibrium was solved for curved panels subjected to uniform lateral outward pressure and uniform shear stress along their four edges and compared against the NACA's experimental results [7]. The Donnell's equation is a partial differential equation for the radial displacement of panel median surface (w), which takes into account the effects of the axial (u), and circumferential (v) displacements. Here, a modified form of the Donnell's equation (Eq. (2)), which was proposed by Batdorf is solved by means of the Galerkin Method [5]. This form of the Donnell's equation is equivalent to its initial form, but has certain advantages in physical interpretations and in ease of solution for different boundary conditions. In the solution of the Donnell's equation, k_s represents the critical shear stress coefficient, and Z is a measure of panel curvature given by:

$$Z = \frac{b^2}{rt}\sqrt{1-\upsilon^2} \tag{1}$$

in which r is the radius of curvature, t is the panel's thickness, and υ is the Poisson's ratio. Accordingly, the modified form of the Donnell's equation for pressured panels under shear forces is:

$$\nabla^4 w + \frac{12Z^2}{b^4}\nabla^{-4}\frac{\partial^2 w}{\partial x^2} + 2k_s\frac{\pi^2}{b^2}\frac{\partial^2 w}{\partial x \partial y} - \frac{prb^2}{\pi^2 D}\frac{\partial^2 w}{\partial y^2} = 0 \tag{2}$$

where p represents the applied lateral pressure. Eq. (2) should be solved to find the critical shear stress coefficient (k_s) as below:

$$k_s = \tau_s \frac{b^2 t}{\pi^2 D} \tag{3}$$

where τ_s is the critical shear stress, and D is the flexural stiffness of the panel.

According to the Galerkin's method, Eq. (2) is solved by expanding the unknown function of w in terms of a suitable set of functions, each satisfying the simply supported boundary conditions. Curved panels either have long straight sides ($\beta = a/b \geq 1.0$), or long circumferential sides ($\beta \leq 1$) (see Fig. 1). The radial displacement (w) for simply supported curved panels with axial sides longer than circumferential sides is written in the form of Eq. (4).

$$w = \sum_{m=1}^{\infty}\sum_{n=1}^{\infty} a_{mn} \sin\frac{m\pi x}{a}\sin\frac{n\pi y}{b} \tag{4}$$

where m and n are the number of buckling half–waves in the axial and circumferential directions respectively. According to the Galerkin's method, the coefficients of a_{mn} should be chosen to satisfy the following equation:

$$\int_0^a \int_0^b \sin\frac{\acute{m}\pi x}{a}\sin\frac{\acute{n}\pi y}{b}\left(\nabla^4 w + \frac{12Z^2}{b^4}\nabla^{-4}\frac{\partial^2 w}{\partial x^2} + 2k_s\frac{\pi^2}{b^2}\frac{\partial^2 w}{\partial x \partial y} - \frac{prb^2}{\pi^2 D}\frac{\partial^2 w}{\partial y^2}\right)dxdy = 0 \tag{5}$$

By substituting Eq. (4) into (5), a set of homogeneous linear algebraic equations is obtained as follows:

$$a_{mn}\left[(m^2 + n^2\beta^2)^2 + \frac{12\beta^4 m^4 Z^2}{\pi^4(m^2 + n^2\beta^2)^2} - \frac{pr\beta^2}{\pi^2 D b^2}n^2\right] + \frac{32\beta^3 k_s}{\pi^2}\sum_{m=1}^{\infty}\sum_{n=1}^{\infty} a_{\acute{m}\acute{n}}\frac{mn\acute{m}\acute{n}}{(m^2 - \acute{m}^2)(n^2 - \acute{n}^2)} = 0 \tag{6}$$

By assigning different values for m and n, two sets of equations, which are associated with the symmetric and anti – symmetric buckling modes, are established. Critical shear stress of panels with particular aspect ratios (β) and curvature parameters (Z) is found via minimizing the value of k_s for which the two sets of equations have a non–vanishing solution.

The above mentioned solution procedure was implemented by use of the Mathematica software [16]. The comparison between this solution and available NACA's experimental results is given in Fig. 2. A very good agreement between the theoretical estimates and experimental results for k_s was observed for both panels under the whole range of applied pressure forces. Though theoretical equations given in this section seem to provide a very reasonable estimate of shear buckling load of curved panels, they do not give any information regarding their postbuckling capacity, which is the subject of next section.

3. NONLINEAR POSTBUCKLING ANALYSIS METHODOLOGY

Finite elements has proven to be a robust tool for analysis of wide range of engineering problems including buckling and postbuckling of plates and shells and is considered in this study for nonlinear investigation of postbuckling behavior of shear curved panels [17-24]. Details of implemented finite element model is discussed in this section. Nonlinear FE analyses were carried out using ABAQUS 6.9 package. A 6– degree of freedom, 4–node quadrilateral doubly curved general–purpose shell element (S4R) was used for modeling, which is appropriate for both thin and thick shells. 33.33×33.33 mm mesh size was chosen per recommendations of another past study [25].

The panels were assumed to be made of an elastic–perfectly plastic structural steel with Young's modulus of 200 GPa and Poisson's ratio of 0.3. The thickness of panels was kept constant and equal to 3 mm. The material's plastic behavior was defined by the von Mises yield criteria and the associated flow rules. The yield stress of the steel is presumed as 327.6 MPa according to the ASTM A36. The out–of– plane displacement of the edge nodes were restrained to simulate simply supported boundary conditions. Also, the translational

degrees of freedom at one corner node of the panels were restricted to prevent any solid displacements.

The implemented nonlinear analyses were divided into two successive steps. In the first step, the normal acting inward or outward pressure was exerted to the surface of the panel, and analyses were conducted by the use of a general load–control static method. In the second step, in–plane shear forces were applied to the edges of pressured panel; and shear buckling and postbuckling responses was monitored. Low frequency dynamic effects were removed using viscous damping[26, 27].

The buckling and postbuckling responses of curved panels frequently involve structural instabilities where the load–displacement path shows a negative stiffness and panels releases strain energy to remain in equilibrium. In such cases, the response of a structural element involves limit–points (maximum and/or minimum loads) rather than bifurcation points, showing both snap–through and snap–back characteristics. Standard static load-control and displacement-control methods are not able to track such behavior and other nonlinear schemes must be used which will be discussed subsequently.

3.1. FE analysis method

Various dynamic and static approaches are available for nonlinear analysis of unstable structures [28]. A standard static solution procedure involves load or displacement increments coupled with full or modified Newton – Raphson iterations. When applying such techniques, severe difficulties can be encountered in the vicinity of limit points, where the load–displacement response becomes horizontal (or vertical). Thus, any attempt to find the true, complete response of a structure with such behavior, including shear curved panel, via standard methods would either fail, or miss some portion of the response and other numerical methods such as Arc-length must be used.

The Arc – length (Riks) method is intended to enable the solution algorithms to pass the limit points. This method works when the applied loading is proportional; i.e., where the

load magnitude is defined by a single scalar parameter. The main essence of the Arc–length method is that the load magnitudes become additional unknowns in the formulations. This approach gives solution regardless of whether the response is stable or unstable [29].

Taking inertia effects into account, dynamic approaches are also applicable to find the load–displacement response of structural elements with unstable response. Although dynamic procedures do not fail in the vicinity of limit points, the true load–displacement response of panels during unstable phases cannot be traced. The conventional FE dynamic procedures can be divided into two main types, namely explicit and implicit; both are used and compared here. The conventional implicit technique adopts a predictor/corrector procedure very similar to the nonlinear static approach. Explicit procedures involve no real equation solving, but there are tight restrictions on the size of the time steps. Despite the unconditionally stable implicit method, the explicit procedure is conditionally stable. The stability limit for an explicit operator is that the maximum time increment must be less than the critical value of the smallest transition time for a dilatational wave to cross any element in the mesh. Applicability of the explicit method is limited to the analysis of short transient problems. If this method is used for quasi – static problems, the inertia effects must be small enough to be neglected [30].

In order to compare the mentioned available analytical methodologies, the shear buckling and postbuckling responses of two curved panels were studied via the four aforementioned methods. All panels have a equal dimension of $1000mm \times 1000mm \times 3mm$, with different curvature parameters of $Z = 5$ and 50.

Applied shear force divided by the yield shear force (V/V_y) against the out–of– plane displacement divided by the wall thickness (w/t) and the circumferential displacement divided by the panel's side dimension (v/a) are presented in Fig. 3. The corresponding nodes for which the displacements are measured are respectively denoted by (9) and (5) in Fig. 1. As it can be seen, the load–displacement responses obtained from different analysis methods, are

exactly similar prior to the buckling load (point A). During the unstable phase of the postbuckling response (from point A to B), the static–general and the dynamic procedures are not capable of tracing the true responses, and snap straight to point B. On the other hand, the Riks method completely demonstrates the snap–through behavior (from point A to B.) It is also observed that after passing point B, the postbuckling equilibrium paths merge and produce almost similar ultimate load capacities (point C). Amongst the above methods, only the Riks method demonstrated the load reductions and softening stages. Thus, it was concluded that only the Riks method enables the true tracing of the complete load–displacement response from the initial linear elastic stage to the ultimate nonlinear strain hardening and softening stages and was used for the rest of this study.

3.2. Validation of FEM procedure

In order to validate the nonlinear FE analysis procedure, a set of analyses was performed to compare the FE results to the theoretical estimations and the available experimental data. The theoretical results were calculated using the Donnell's equation of equilibrium as described in section 2. A set of tests was carried out by NACA to evaluate the effect of normal pressures on the critical shear and compressive stresses of curved sheets [7, 8]. The experimental data in this section are extracted from those tests. The dimensions of the panels are given in Table 1. Specimens were made of aluminum ST-24 alloy with the Young's modulus of 68.95 GPa, Poisson's ratio of 0.3, and yield stress of 372.32 MPa.

The panels were loaded and analyzed in two subsequent steps similar to the actual tests. In the first step, outward pressures were applied to the surface of the panel and a nonlinear general static analysis was carried out. Subsequently, in the second step, shear forces were uniformly applied to the edges and a nonlinear Riks analysis was conducted.

The results are presented in Figs. 4 and 5. Fig. 4 shows the load-displacement response of three studied panels under various lateral pressure loads which was used to estimate their buckling shear stress. These values are compared to those predicted by Donnell

equation and also NACA test results in Fig. 5. As it can be seen in Fig. 5, for panel S1, which has the greatest curvature parameter among three ($Z = 108$), both Donnell equation and FE analysis predicted the test results very well up to lateral pressure of $20kPa$, however Donnell equation underpredicts the buckling stress under greater lateral pressure forces. For panel S2 and S3, which have smaller curvature parameters, FE analysis and test results are in a very good agreement while Donnell Equation again underpredicted the buckling load for most samples. Considering the good agreement between FE method and NACA test results for various curvatures and lateral pressure forces, postbuckling behavior of curved panels was investigated using FE method and results are discussed in the next section.

4. RESULTS AND DISCUSSION

The influence of the lateral pressures on the shear buckling and postbuckling behavior of curved panels is discussed in this section. Four curved panels with various curvature parameters of $Z = 5, 15, 50$ and 150, aspect dimensions of $1000mm \times 1000\,mm$ and wall thickness of 3 mm were considered. The influence of both uniform and hydrostatic outward and inward pressures ranging from 1 kPa to 10 kPa was studied. For panels subjected hydrostatic pressure, the loads were linearly distributed from zero to a maximum specified magnitude. Lateral pressures and in–plane shear loads were applied in two subsequent stages; and in each stage, a full nonlinear FE analysis was performed.

4.1. Inward pressures

The shear buckling and postbuckling behavior of curved panels in the presence of the inward lateral pressures is presented in Figs. 6 to 12. According to Figs. 6 and 7, the panels which had very low ($Z = 5$) and low ($Z = 15$) curvatures did not exhibit any buckling bifurcation points due to the presence of the inward pressures. As a result, the subsequent post–critical load reductions disappeared and panels became more stable at the buckling load levels. Therefore, a further growth of the shear force was observed beyond the theoretical load

levels. In addition, there was no considerable reduction in the ultimate load–bearing capacities. The initial deflections, which are induced by the inward pressure, disturb the membrane action of the panels; thus, no strain energy was conserved before the buckling and the snap–through point was eliminated from the response.

In Fig. 8 the load–displacement response of the moderately curved panel ($Z = 50$) is given. It is observed that for small inward pressures (1 kPa), the panel behaved similar to the case of pure shear; exhibiting snap–through unstable buckling, with a considerable reduction in the buckling load. In contrast, when the inward pressure was increased to 5 kPa or more, the behavior of the moderately curved panel became stable similar to the low curved panels. Fig. 9 shows the out–of–plane deflection contours of the two panels under pure shear loads and a combination of shear and 5kPa inward pressure. Accordingly, the buckling mode shape was changed from two half–waves in the case of the pure shear to one half–wave in the presence of inward pressure.

Fig. 10 depicts the load–deflection response of the highly curved panel ($Z = 150$). In this case, unlike the less curved panels, the ultimate load was considerably reduced due to the increasing presence of inward pressures. The failure mode was associated with the occurrence of unstable buckling; and the large amount of the released strain energy most likely prevented the hardening effects. Fig. 11 compares the buckling mode shapes of the panel in three mentioned loading conditions. As it can be seen, the buckling mode shape of the pressured panels was similar to the case of pure shear.

Fig. 12 compares the load–deflection response of panels subjected to a combination of in–plane shear forces and different magnitudes of inward hydrostatic pressures. It is observed that there was no bifurcation point in the slightly curved panels ($Z = 5, 15$); whereas, in panels with greater curvature parameter ($Z = 50, 150$), the bifurcation points and the subsequent snap–through and hardening stages were distinctly apparent.

In order to investigate the influence of the aspect ratio on the stability behavior of curved panels, the results of twelve FE analyses under the two different loading conditions (pure shear loads vs. combined shear and hydrostatic inward pressures) are compared in Figs. 13-15. It is observed that the ultimate capacity was considerably decreased with the aspect ratio regardless of the curvature parameter. However, the unstable buckling was clearly evident in all the panels with $Z = 50, 150$.

4.2. Outward pressures

The results for panels subjected to outward lateral pressures are given in Figs. 16 to 23. According to Figs. 16 and 17, there was no distinct buckling point in the response of panels with very low ($Z = 5$) and low ($Z = 15$) curvature. On the other hand, the outward normal pressure significantly increased buckling load of panels with greater curvature parameter ($Z = 50$) (see Fig. 18). This increase could be attributed to the interaction of the shear induced compressive membrane stresses and the pressure induced tensile membrane stresses. The snap–through phenomenon was not generally observed in panels under hydrostatic outward pressures. But, the snap–back phenomenon was observed in panels under uniform outward pressures. It is also realized that the ultimate loads of panels under the effect of uniformly distributed outward pressure were significantly increased. The difference between the buckling behavior of panels under the effect of uniform and hydrostatic pressures is due to the difference between the first and the second shear buckling eigenmodes as depicted in Fig. 19. In addition, Fig. 20 depicts the buckling mode shapes of panels under the effect of various load combinations. According to Figs. 19 and 20, the first buckling eigenmode was observed in panels under pure shear loads and panels under the combined action of in–plane shear loads and hydrostatic pressures. However, the second buckling eigenmode was observed in panels under the combined action of in – plane shear loads and uniform pressures.

Fig. 21 illustrates the load – displacement curves of panels with the curvature parameter of $Z = 150$. It is observed that the outward normal pressure did not significantly increase critical loads. The von Mises stress contours and the buckling mode shapes of panels under pure shear loads and combined shear and hydrostatic outward pressures are compared in Fig. 22. As depicted, three buckling half – waves were observed and tension fields were clearly formed in both cases followed by the material softening stage. In Fig. 23, the comparison between the load – deflection response of panels having different curvatures under combined action of hydrostatic outward pressures and in – plane shear forces is presented. It is observed that the initial stiffness of panels were similar up to the buckling load limit.

The effects of the aspect ratio on the panels' buckling and postbuckling behavior under the action of outward pressures are depicted in Figs. 24 to 26. It is observed that in panels with $Z = 15$ and the aspect ratios of 1 and 1.5, the ultimate loads were increased due to the presence of the hydrostatic pressures. This increase could be due to the pressure induced tensile stresses counteracting the shear induced compressive stresses. However, in the panels with higher aspect ratios, the ultimate capacity was decreased. Similar results for the panels with $Z = 50$ show that in panels with the aspect ratios 1, 1.5 and 2, the critical shear stress was significantly increased by the outward pressures. In the panel with the aspect ratio of 2.5, the bifurcation point was not distinctive and the ultimate load was slightly increased under the influence of hydrostatic pressure. It is concluded that the hydrostatic outward pressures prevented the panels with the aspect ratio of 2.5 from buckling. Fig. 26 presents the results for panels with the curvature parameter of $Z = 150$. It is also evident that the ultimate capacity was increased due to the influence of the hydrostatic outward pressures, regardless of the panel aspect ratio. However, the panel with the aspect ratio of 2 showed the maximum increase in the ultimate capacity.

Finally, the differences between the effects of inward and outward lateral hydrostatic pressures on the shear buckling behavior of curved panels are depicted in Fig. 27. The variation of the applied shear loads against the corner circumferential displacement of square panels having the curvature parameters of $Z = 5, 15, 50, 150$ are presented in Fig. 27. It is observed that, in general, outward pressures increased the shear load capacity of the curved panels; while inward pressures decreased their capacity. Such effects were negligible in shallow curved panels; whereas in highly curved panels, the effects were considerable. In the panel with $Z = 50$, the outward pressures considerably increased the elastic buckling capacity, while the inward pressures removed the buckling phenomenon. In the highly curved panels ($Z = 150$), outward pressures slightly increased the buckling capacity, but inward pressures significantly decreased them.

5. Conclusions

The shear buckling and postbuckling behavior of thin curved steel panels subjected to gradually increasing in–plane shear forces in the presence of inward and outward normal pressures were investigated. The main concluding remarks based on the considered cases in this study are as follows:

- Amongst the various available nonlinear FE analysis methods, the Arc length Riks method can more realistically trace the complete load–displacement response of curved panels. Both the stable and unstable buckling phenomena, as well as all strain hardening and softening phases, are well predicted by the use of Riks method.
- Small amounts of inward pressures eliminate the snap–through shear buckling and the post unstable buckling softening stages in shallow curved panels. The shear capacity continued to increase after the theoretical critical loads. In moderately curved panels, however, small amounts of pressures did not alter their buckling behavior.
- The magnitude of inward pressures required to influence the shear buckling and postbuckling behavior of curved panels, depends on their curvature. Panels with

greater curvature parameter require higher pressures. The buckling mode shapes of curved panels are also considerably affected by the amount of pressures.

- The ultimate shear capacity of highly curved panels is considerably reduced by the increasing presence of inward pressures. The failure modes of such panels are associated with the occurrence of unstable buckling, and the amount of the released strain energy prevents hardening effects.
- Increasing the aspect ratio of curved panels, considerably decreases their ultimate shear capacity. This is regardless of the radius of curvature, although signs of unstable buckling are clearly evident in moderate to highly curved panels.
- In general, outward pressures increase, and inward pressures decrease the shear buckling capacity of curved panels; the magnitude of such changes increase with the curvature parameter. Inward pressures can remove the bifurcation points, and make panels behave like imperfect flat panels. Outward pressures make the buckling phenomenon to be more stable.

Nomenclature

a, b	length and width of the curved panel, respectively (mm)
a_{mn}	coefficients in deflection function
β	aspect ratio of the panel (=a/b)
D	flexural stiffness of the curved panel per unit length (=$\frac{Et^3}{12(1-\upsilon^2)}$)
k_s	critical shear stress coefficient ($=\tau_s \frac{b^2 t}{\pi^2 D}$)
m, n	number of buckling half – waves in the axial and circumferential directions, respectively
υ	Poisson's ratio
p	applied lateral pressure (kPa)
r	radius of curvature of the curved panel
t	thickness of the curved panel (mm)
u, v, w	displacement of points on median surface of the curved panel in axial (x), circumferential (y) and radial (z) directions, respectively
V	applied shear load

V_y shear yield load

x, y, z axial, circumferential and radial coordinates, respectively; shown in Fig. 1

Z curvature parameter of the panel ($= \frac{b^2}{rt}\sqrt{1-v^2}$)

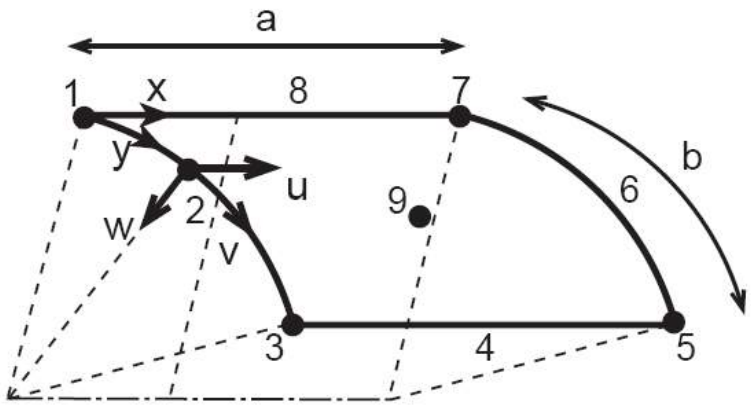

General view

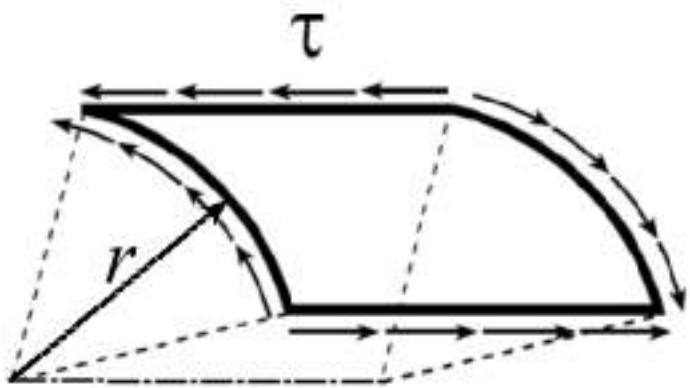

In-plane shear forces

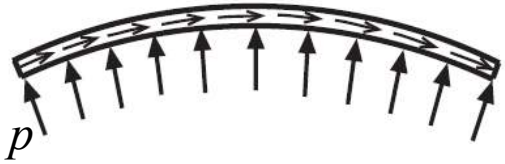

Outward uniform pressure

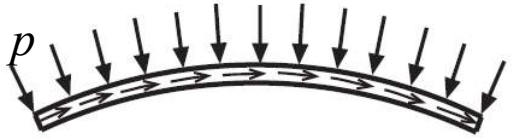

Inward uniform pressure

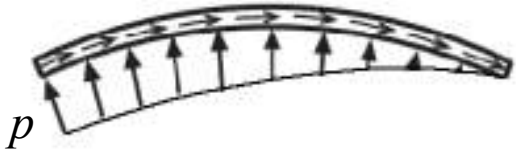

Outward hydrostatic pressure

Outward hydrostatic pressure

Fig. 1 General view and loading conditions

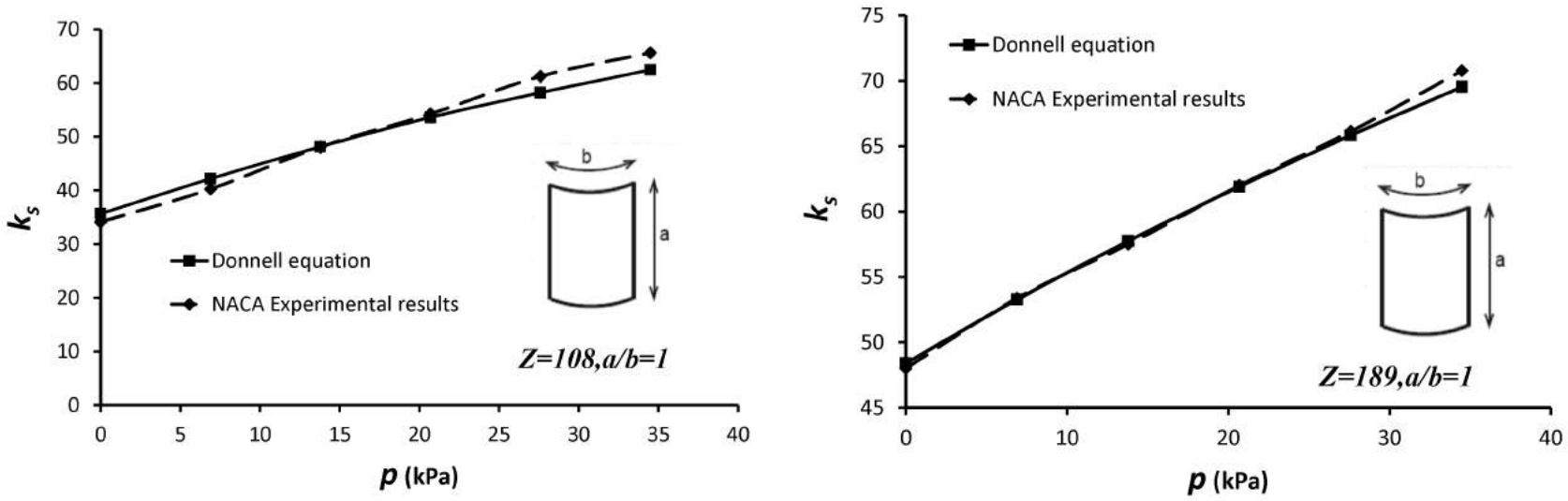

Fig. 2 Elastic shear buckling coefficient versus outward normal pressures for two typical panels

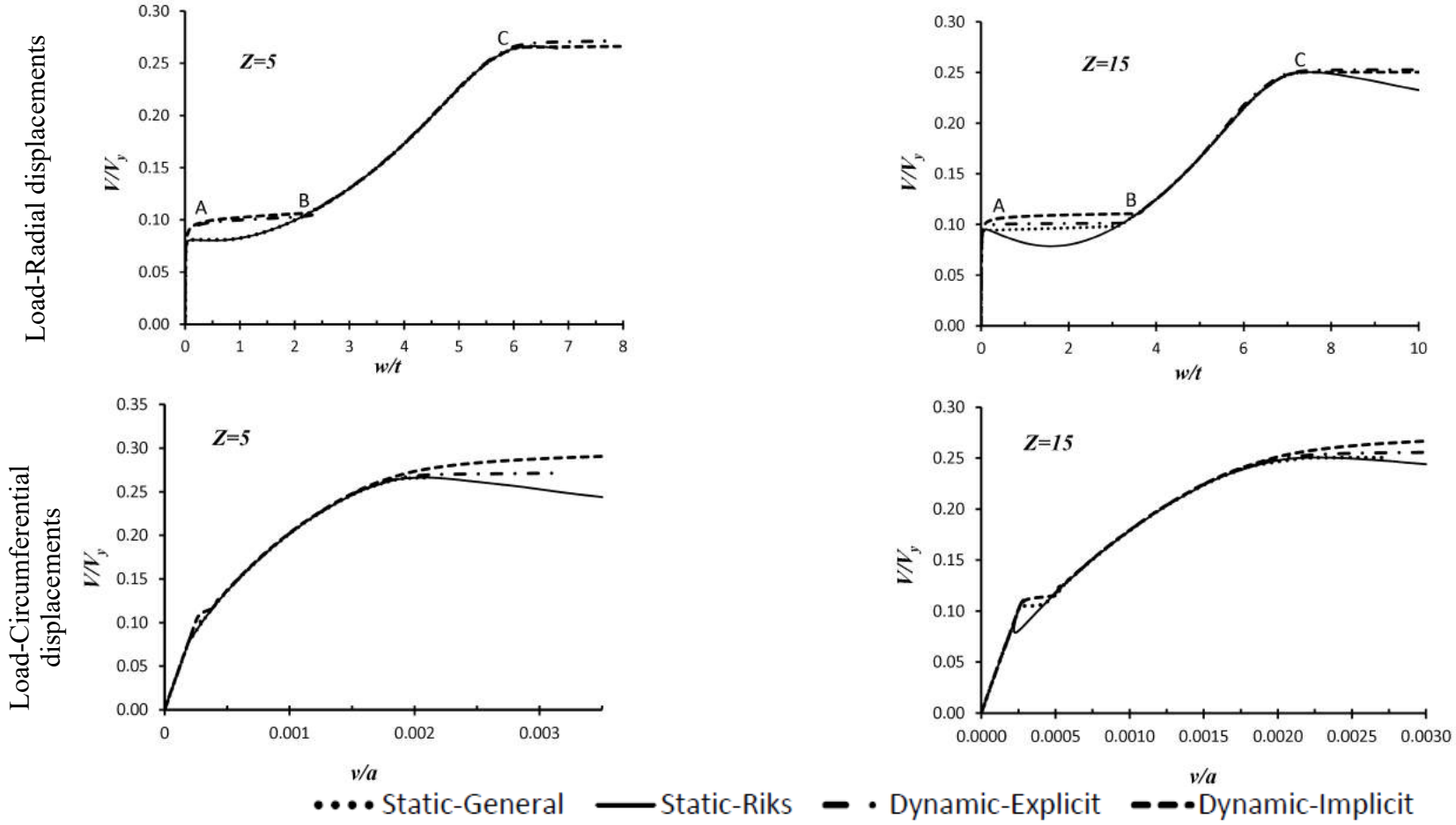

Fig. 3 Load – displacement curves for square panels with various curvatures

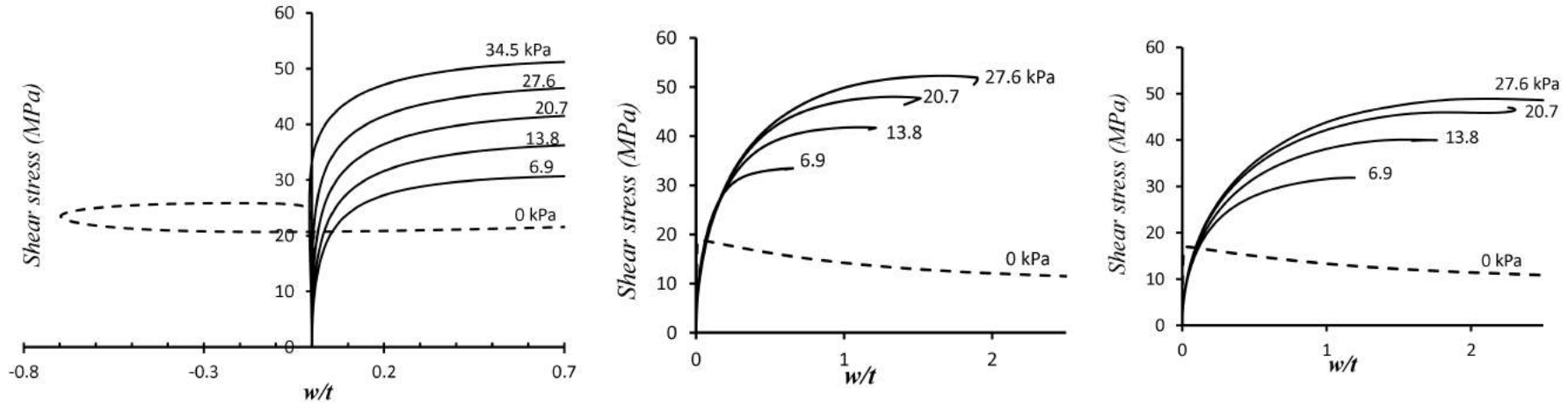

(a) S1 (b) S2 (c) S3

Fig .4 Middle node displacements versus applied shear force

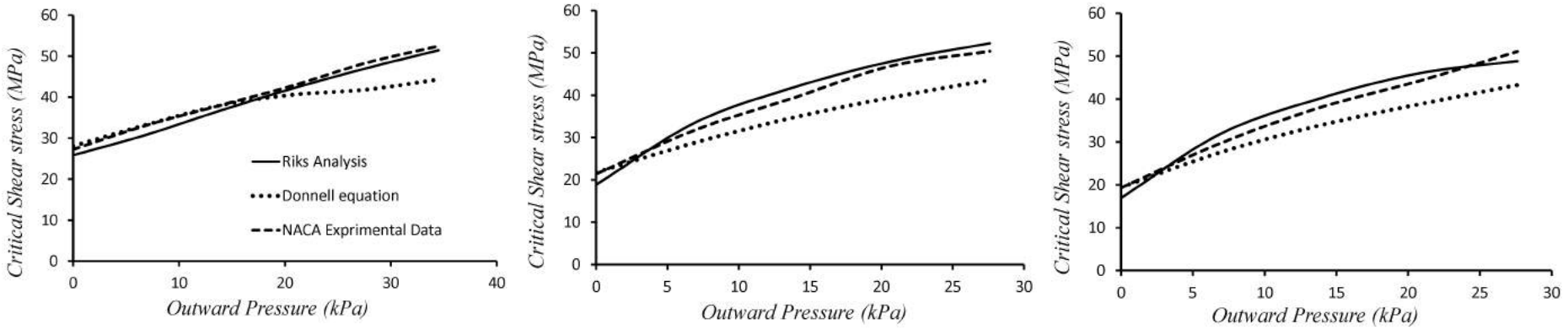

(a) S1 (b) S2 (c) S3

Fig. 5 Critical shear stress versus normal pressure stress

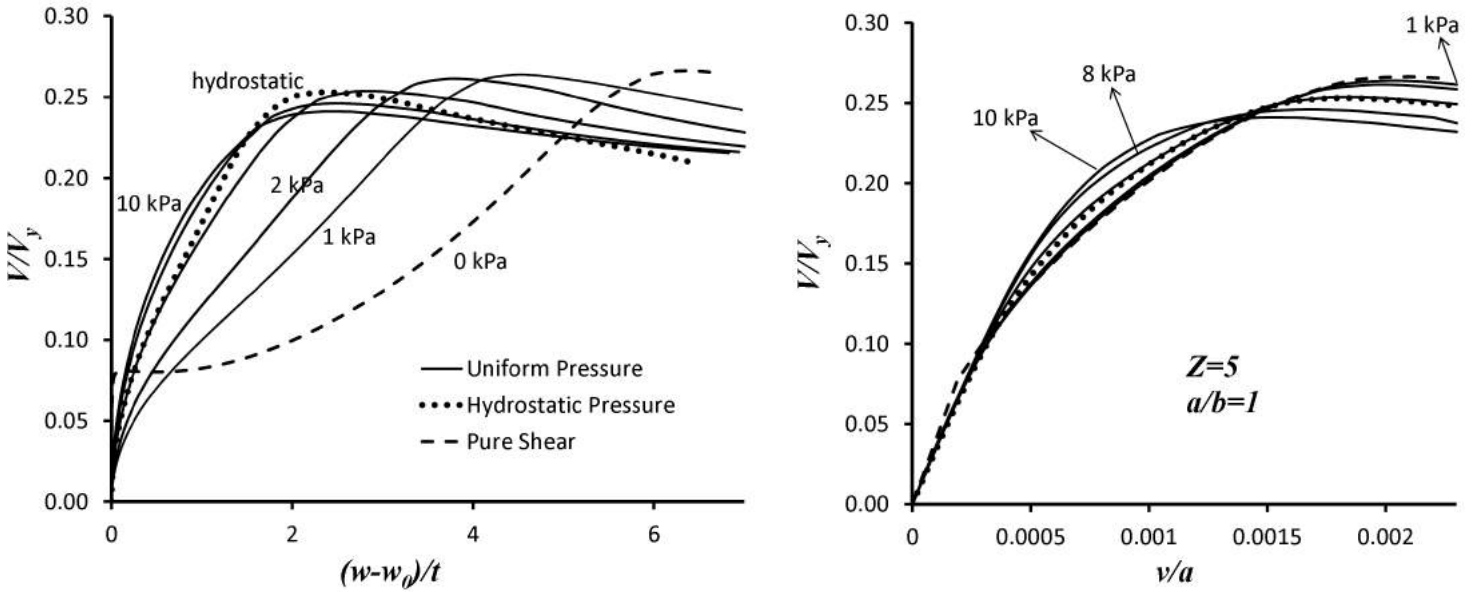

(a) Radial displacement - Middle node (b) Circumferential displacement - Corner node

Fig. 6 Load-displacement curves for panels with *Z=5* and *a/b=1* – Inward pressures

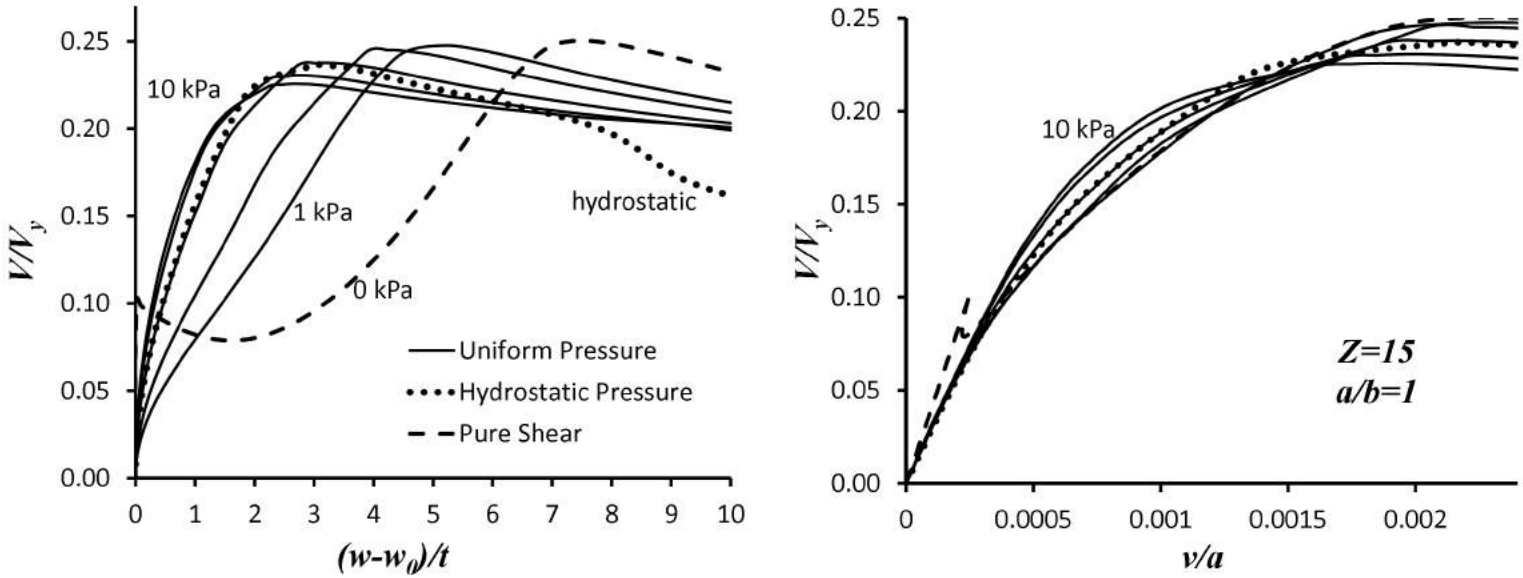

(a) Radial displacement - Middle node (b) Circumferential displacement - Corner node

Fig. 7 Load-displacement curves for panels with *Z=15* and *a/b=1* – Inward pressures

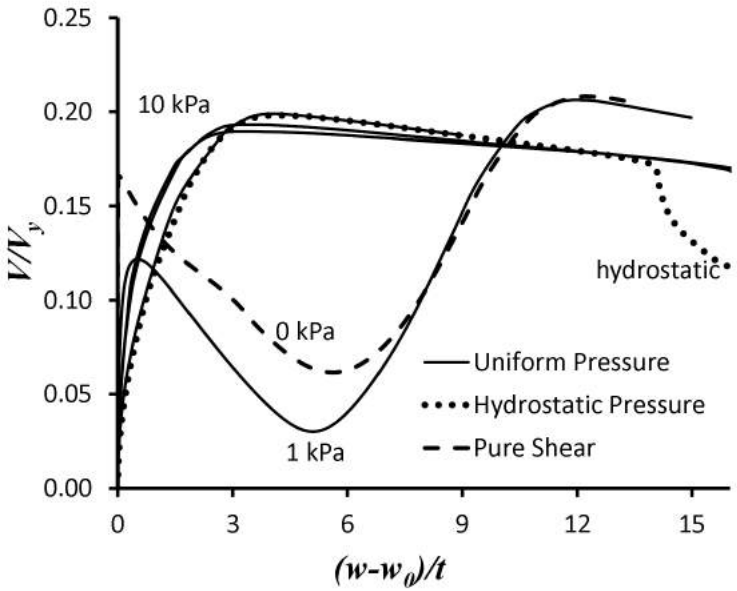

(a) Radial displacement - Middle node

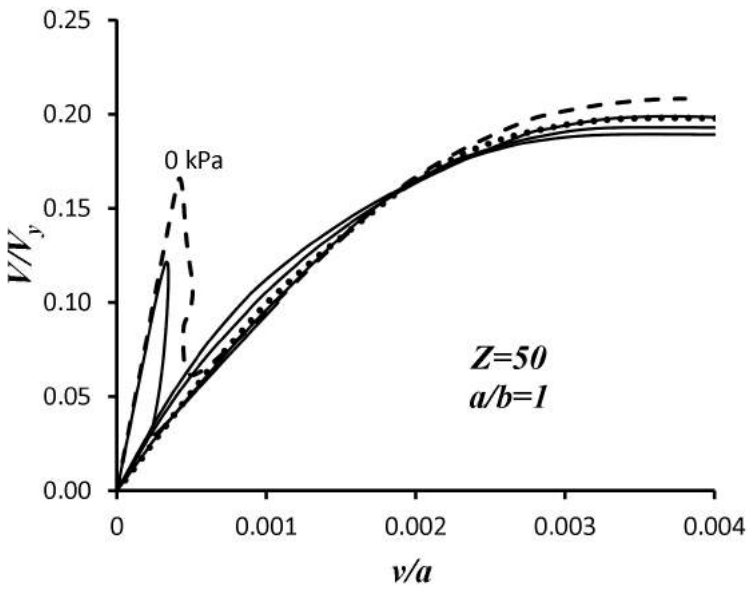

(b) Circumferential displacement - Corner node

Fig. 8 Load-displacement curves for panels with *Z=50* and *a/b=1* – Inward pressures

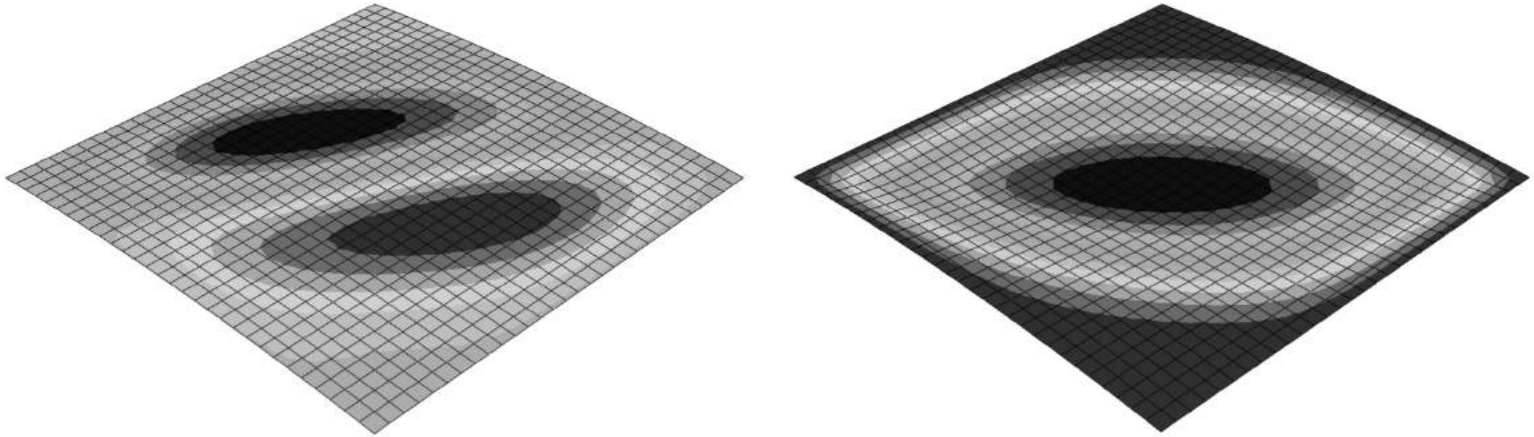

(a) Pure shear

(b) Combined shear and 5 kPa inward normal pressure

Fig. 9 Buckling mode shapes for panels with *Z=50*

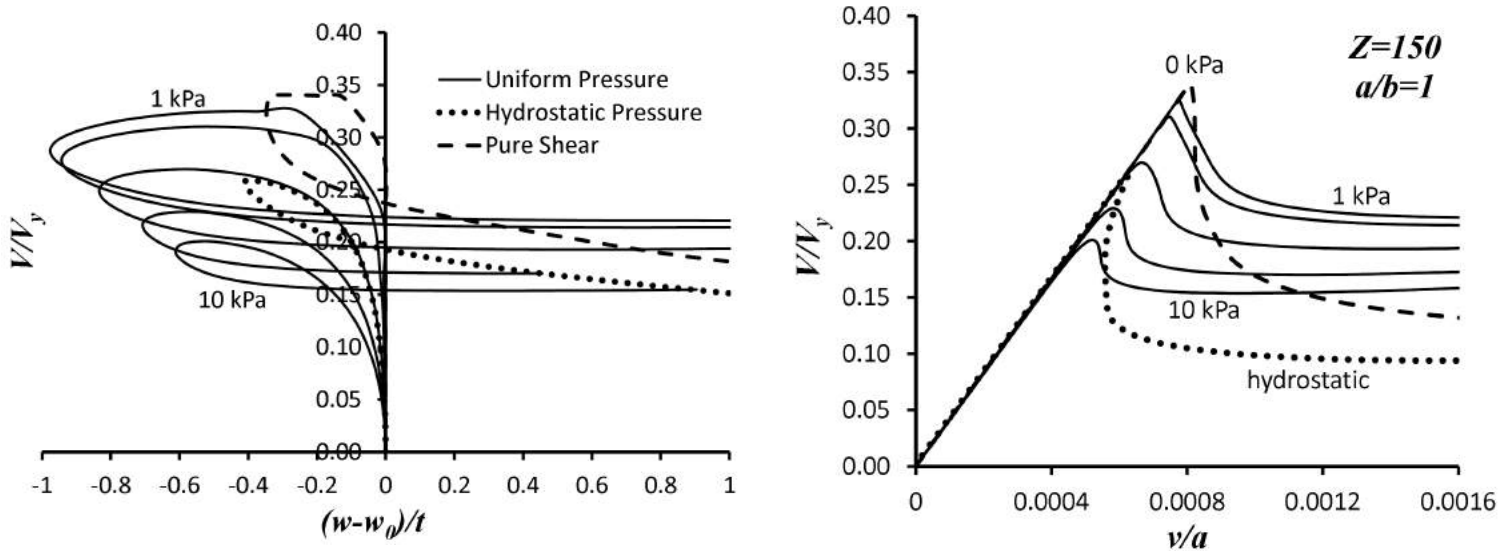

(a) Radial displacement - Middle node (node 9) (b) Circumferential displacement - Corner node (node 5)

Fig. 10 Load-displacement curves for panels with *Z=150* and *a/b=1* – Inward pressures

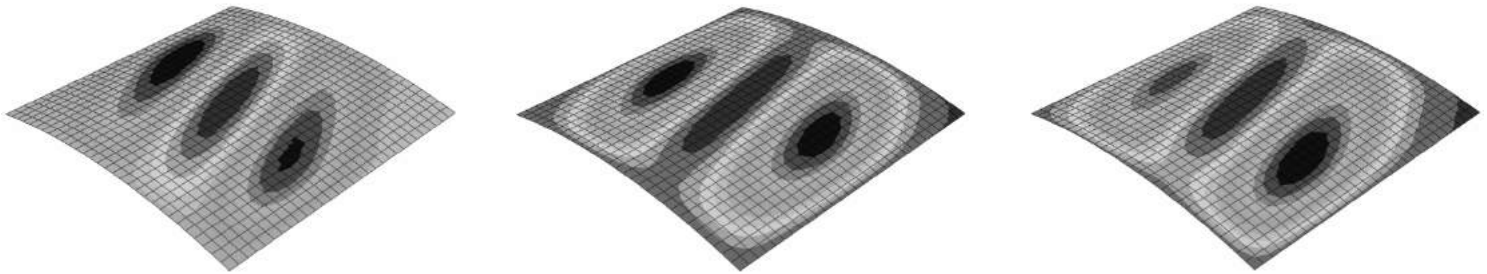

(a) Pure shear

(b) Combined shear and 10 kPa uniform inward normal pressure

(c) Combined shear and hydrostatic inward normal pressure

Fig. 11 Buckling mode shape for panels with *Z=150*

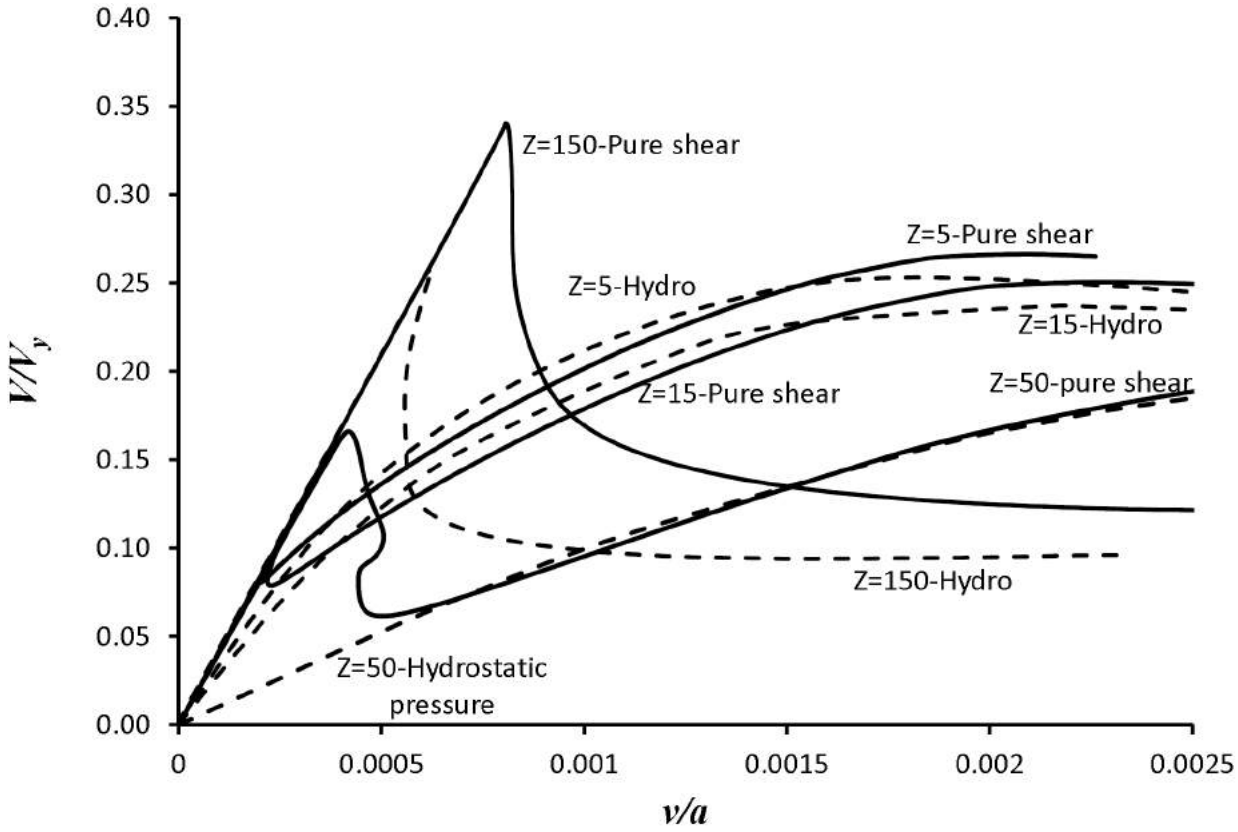

Fig. 12 Comparison of load-displacement curves for different panels under inward pressures

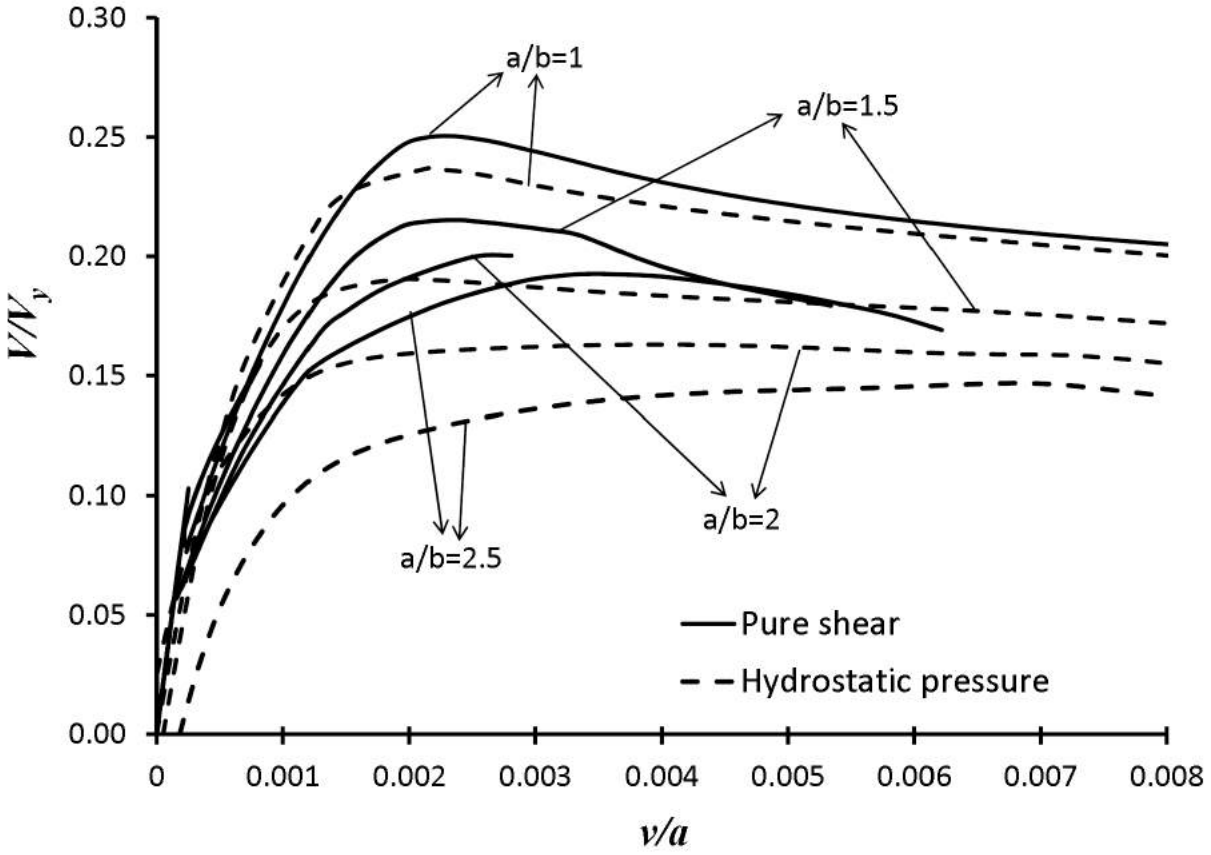

Fig. 13 Shear-circumferential displacement curves for panels with *Z=15* – Inward pressures

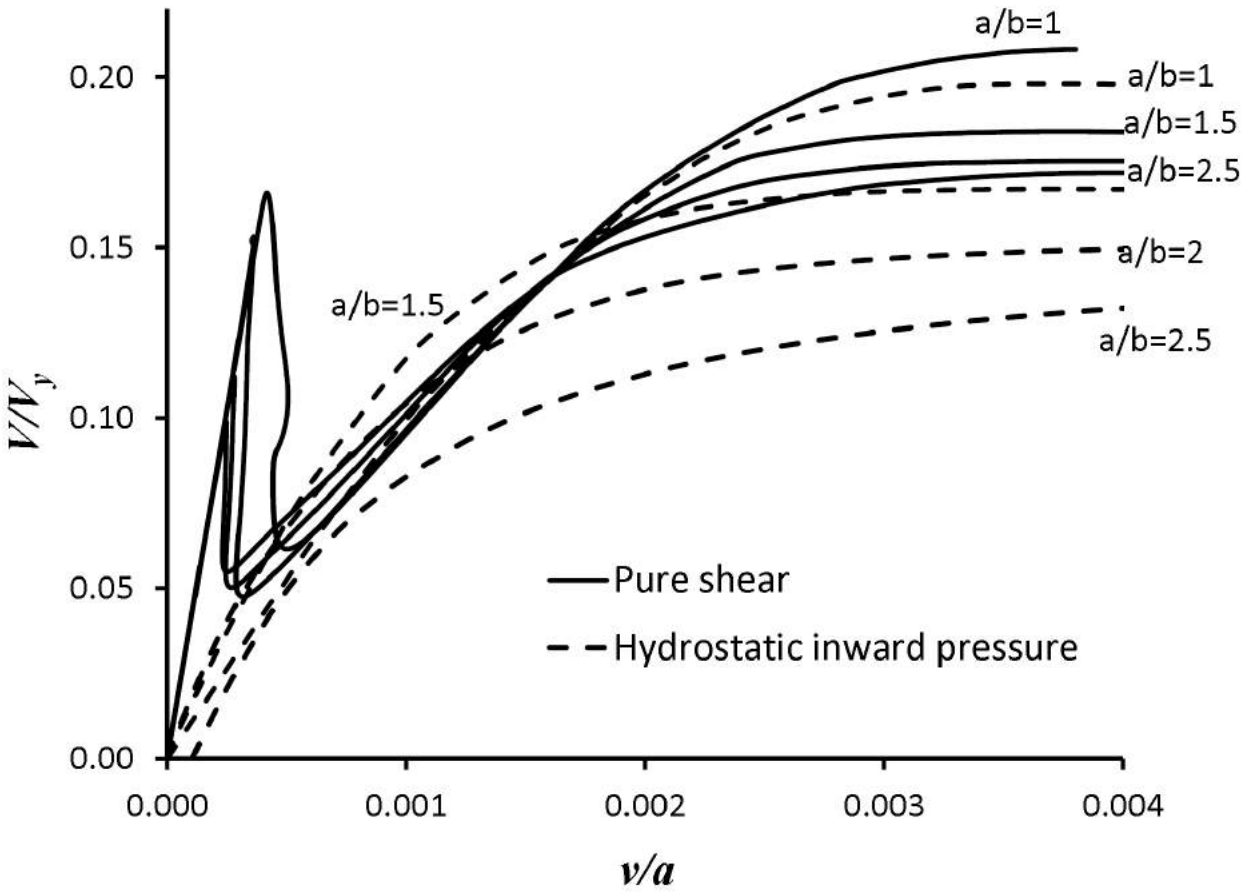

Fig. 14 Shear-circumferential displacement curves for panels with *Z=50* – Inward pressures

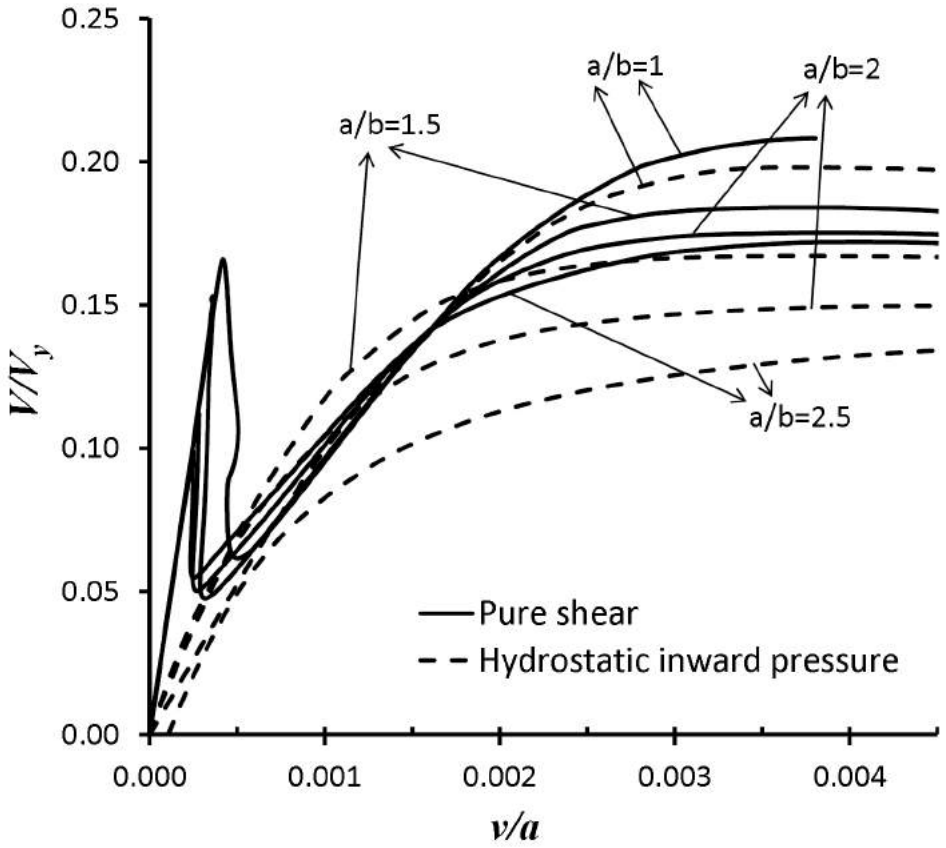

Fig. 15 Shear-circumferential displacement curves for panels with *Z=150* – Inward pressures

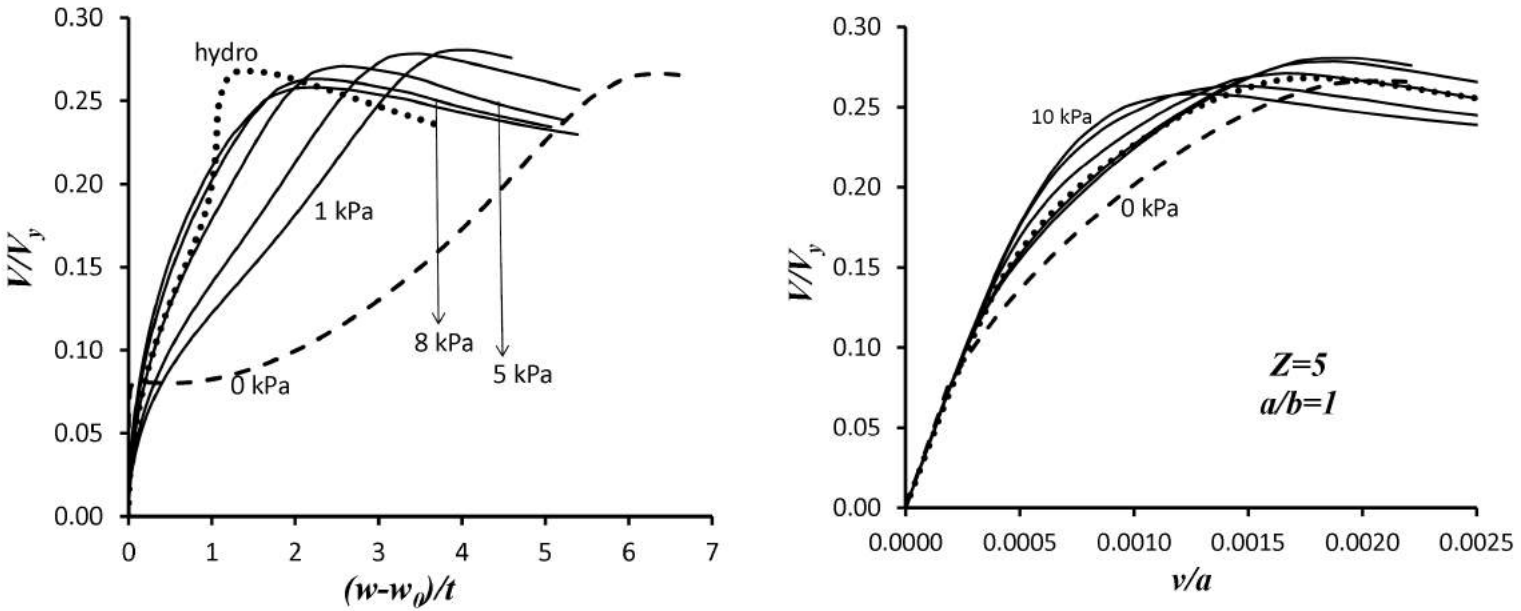

(a) Radial displacement - Middle node (node 9) (b) Circumferential displacement - Corner node (node 5)

Fig. 16 Load-displacement curves for panels with *Z=5* and *a/b=1* – Outward pressures

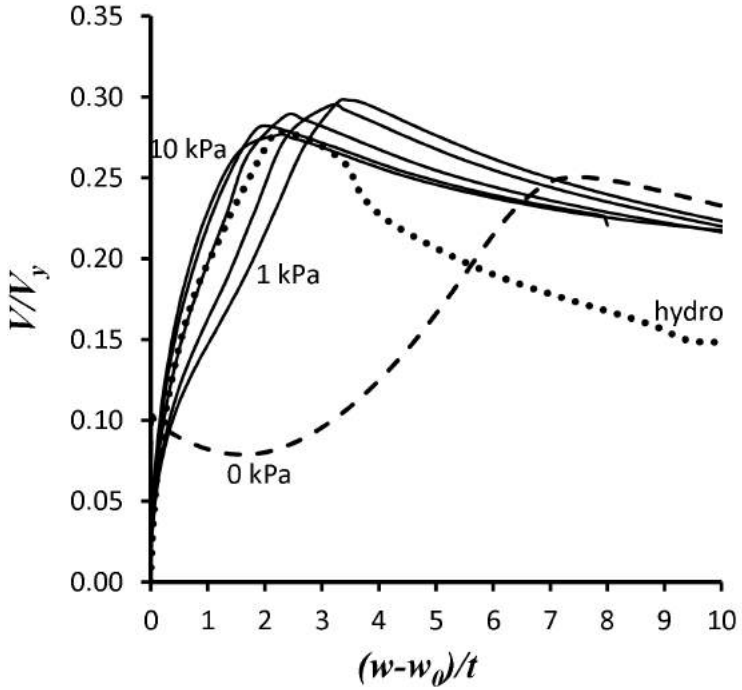

(a) Radial displacement - Middle node (node 9)

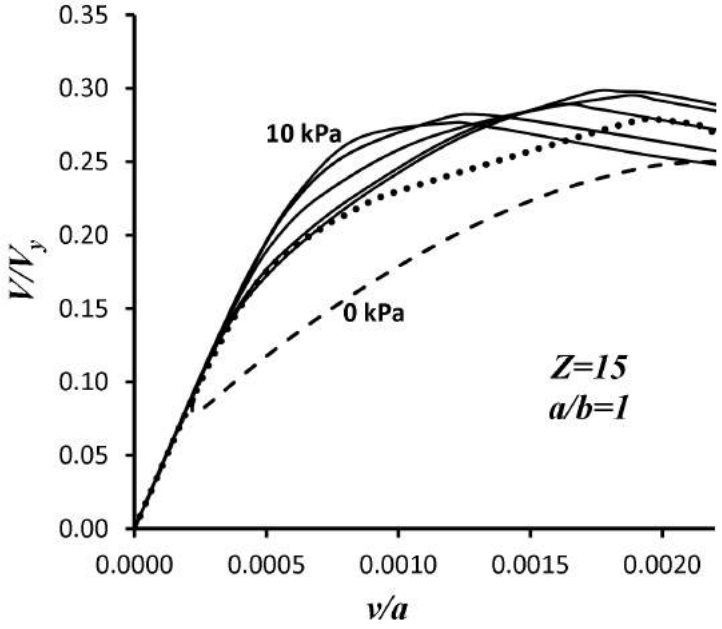

(b) Circumferential displacement - Corner node (node 5)

Fig. 17 Load-displacement curves for panels with *Z=15* and *a/b=1* - Outward pressures

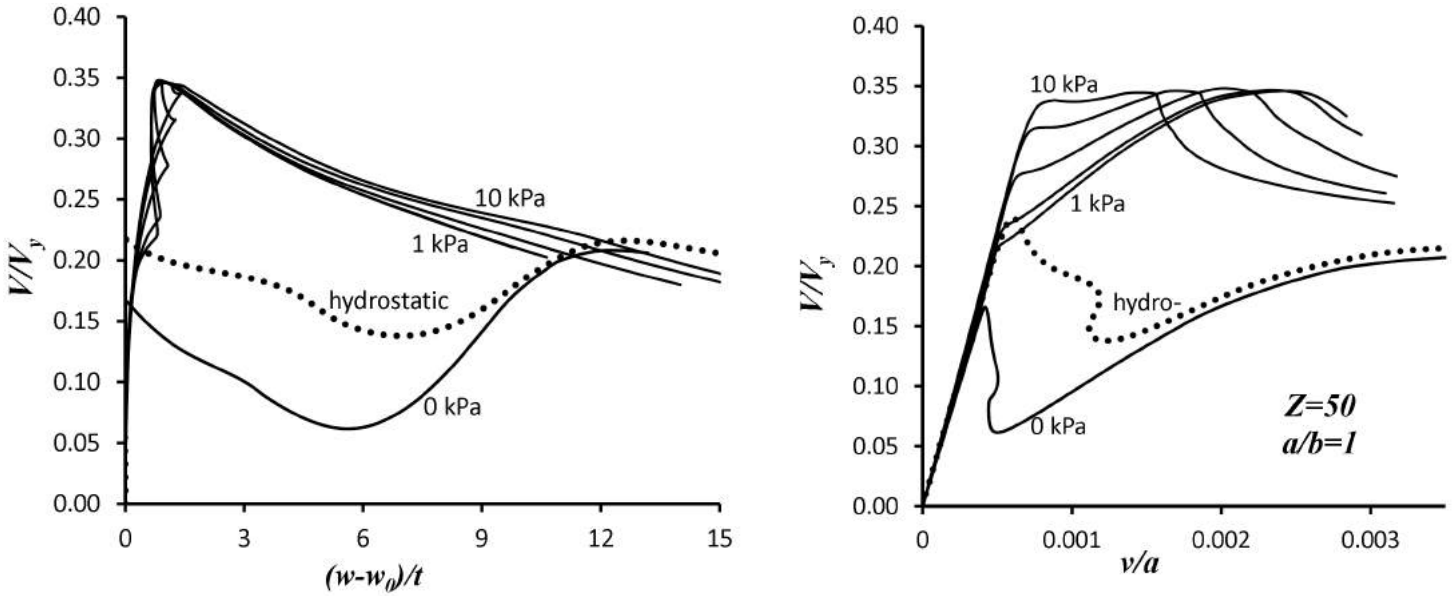

(a) Radial displacement - Middle node

(b) Circumferential displacement - Corner node

Fig. 18 Load/displacement curves for panels with *Z=50* and *a/b=1* - Outward pressures

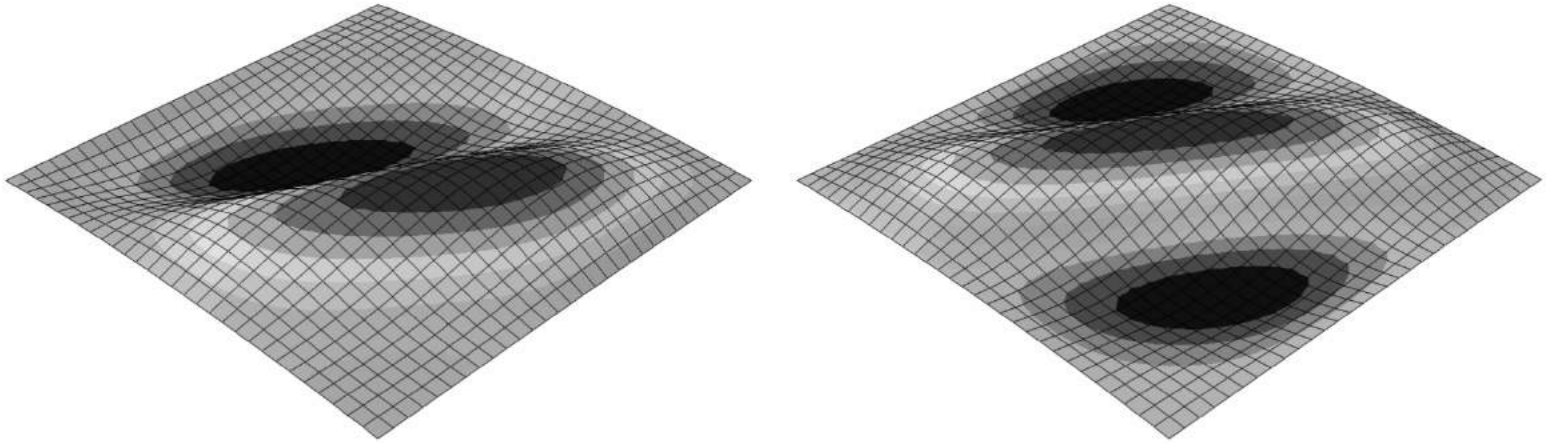

(a) 1st eigenmode b) 2nd eigenmode

Fig. 19 Eigenmodes of panels with Z=50 under pure shear

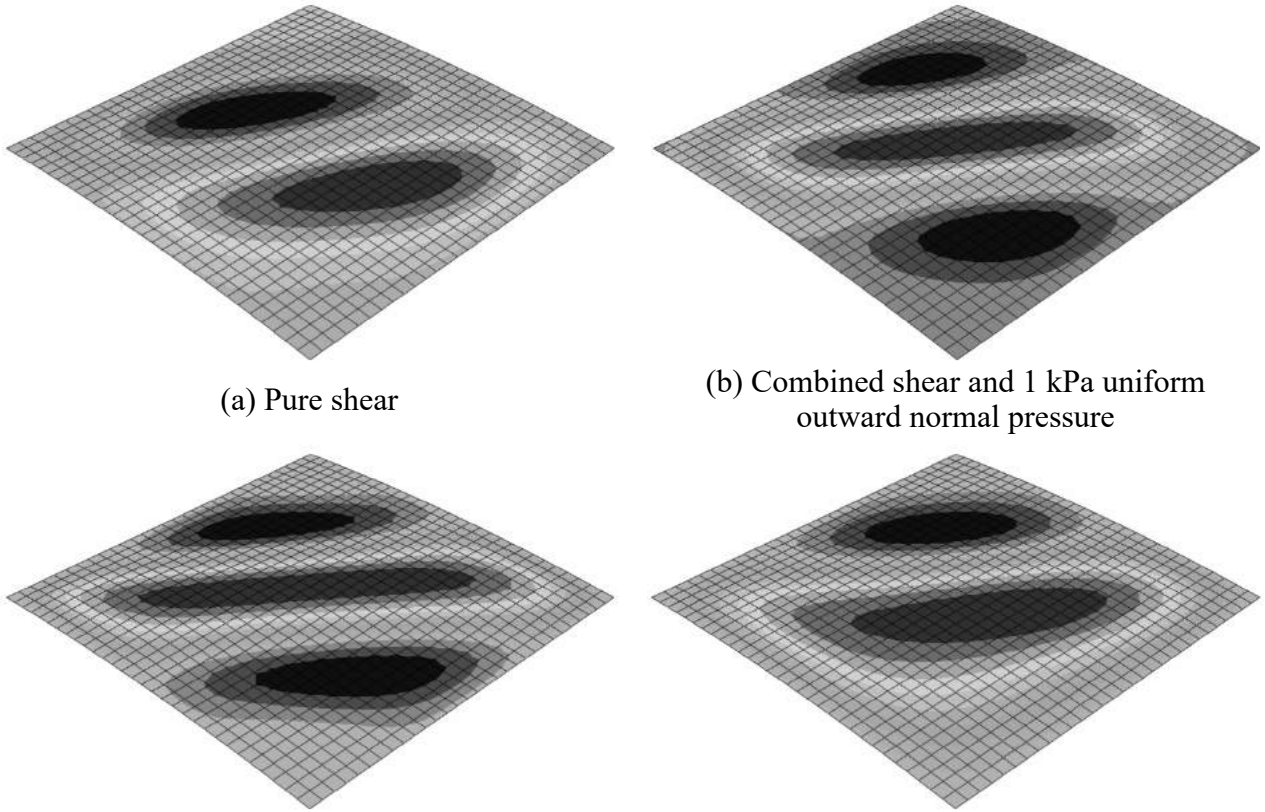

(a) Pure shear

(b) Combined shear and 1 kPa uniform outward normal pressure

(c) Combined shear and 10 kPa uniform outward normal pressure

(d) Combined shear and hydrostatic outward normal pressure

Fig. 20 Buckling mode shapes of panels with Z=50

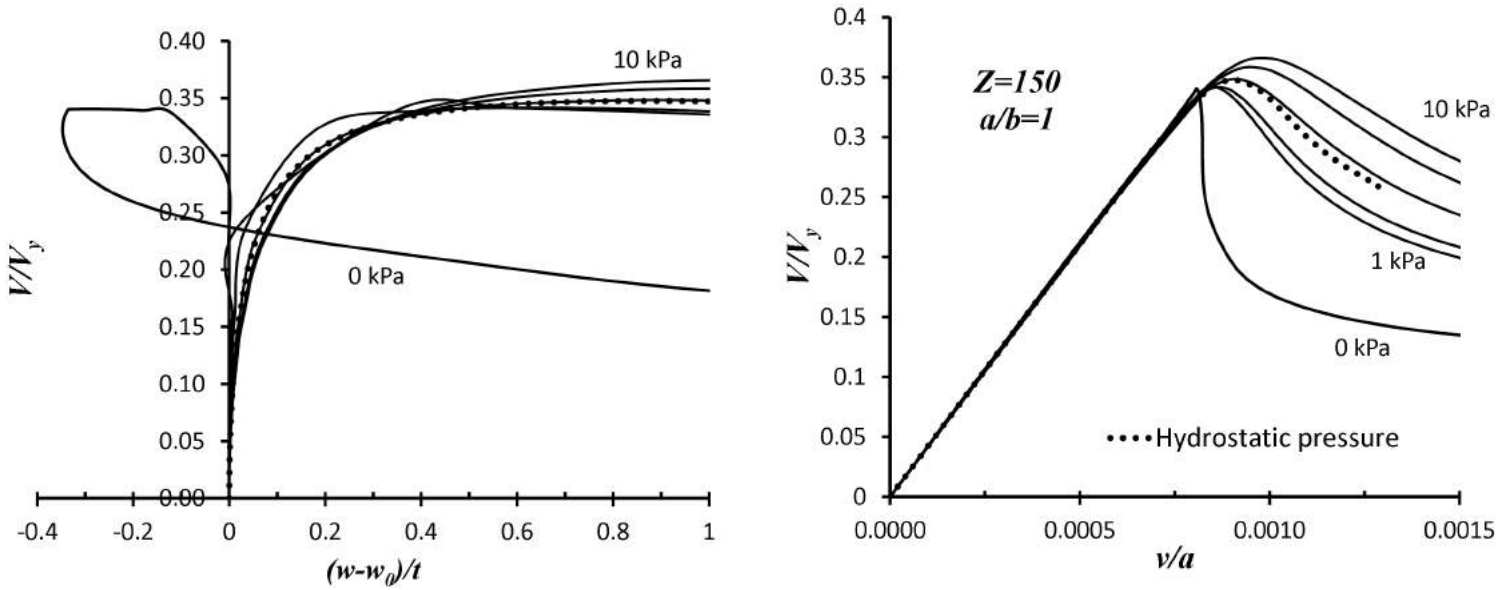

(a) Radial displacement - Middle node

(b) Circumferential displacement - Corner node

Fig. 21 Load/displacement curves for panels with *Z=150* and *a/b=1* - Outward pressures

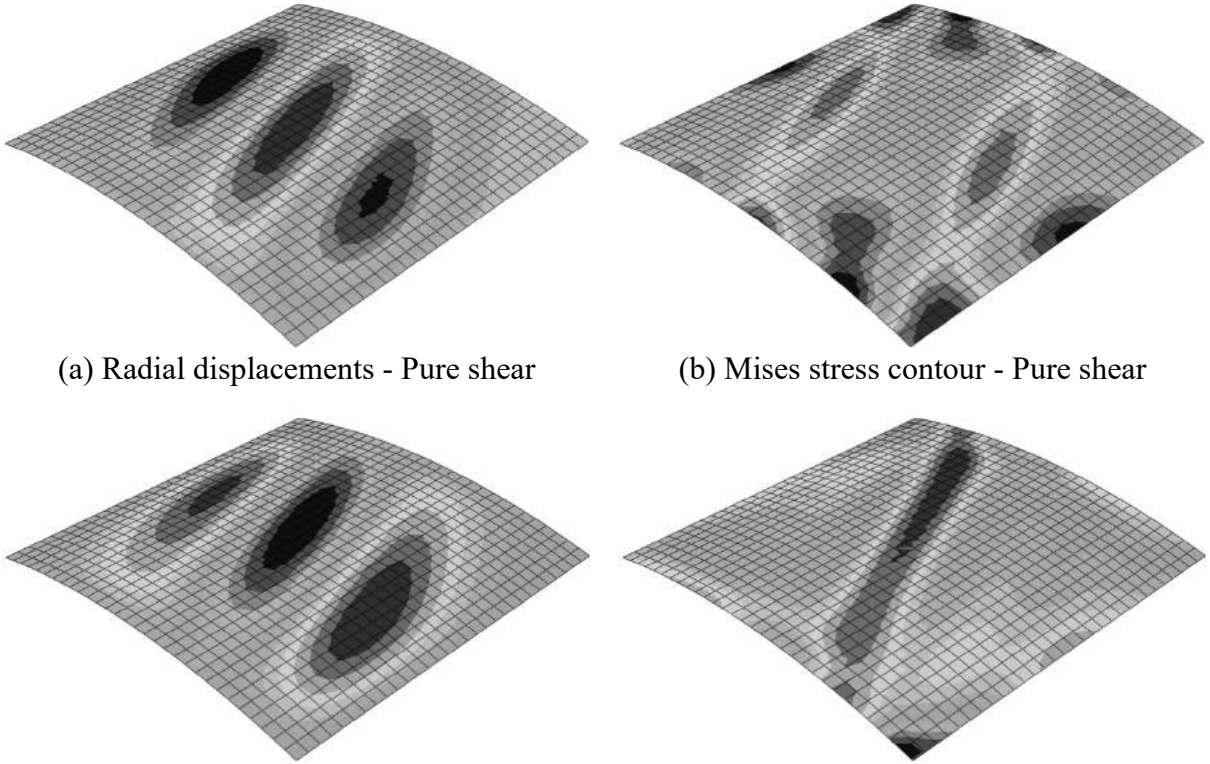

(a) Radial displacements - Pure shear

(b) Mises stress contour - Pure shear

(c) Radial displacements - combined shear and hydrostatic pressure

(d) Mises stress contour - combined shear and hydrostatic pressure

Fig. 22 Buckling mode shapes of panel with *Z=150*

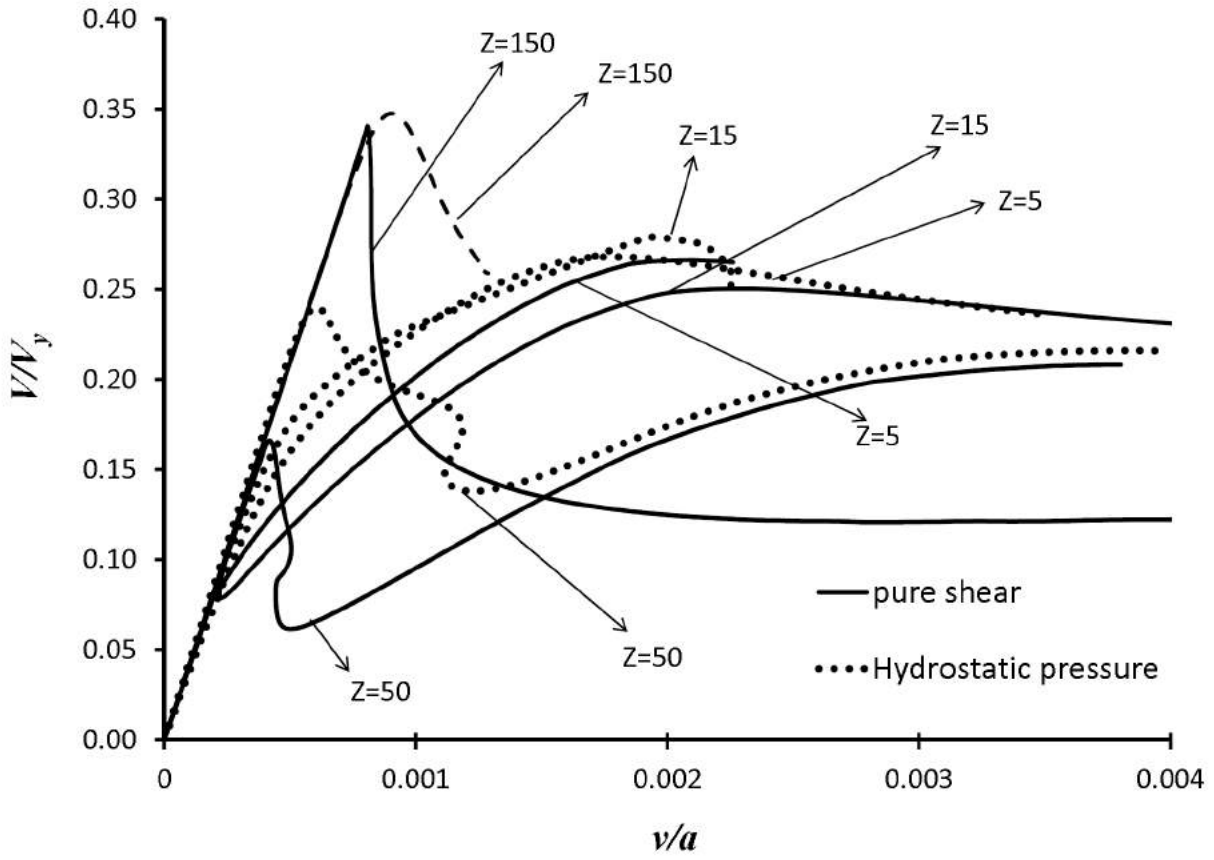

Fig. 23 Comparison of shear – circumferential displacement curves for different panels - Outward pressures

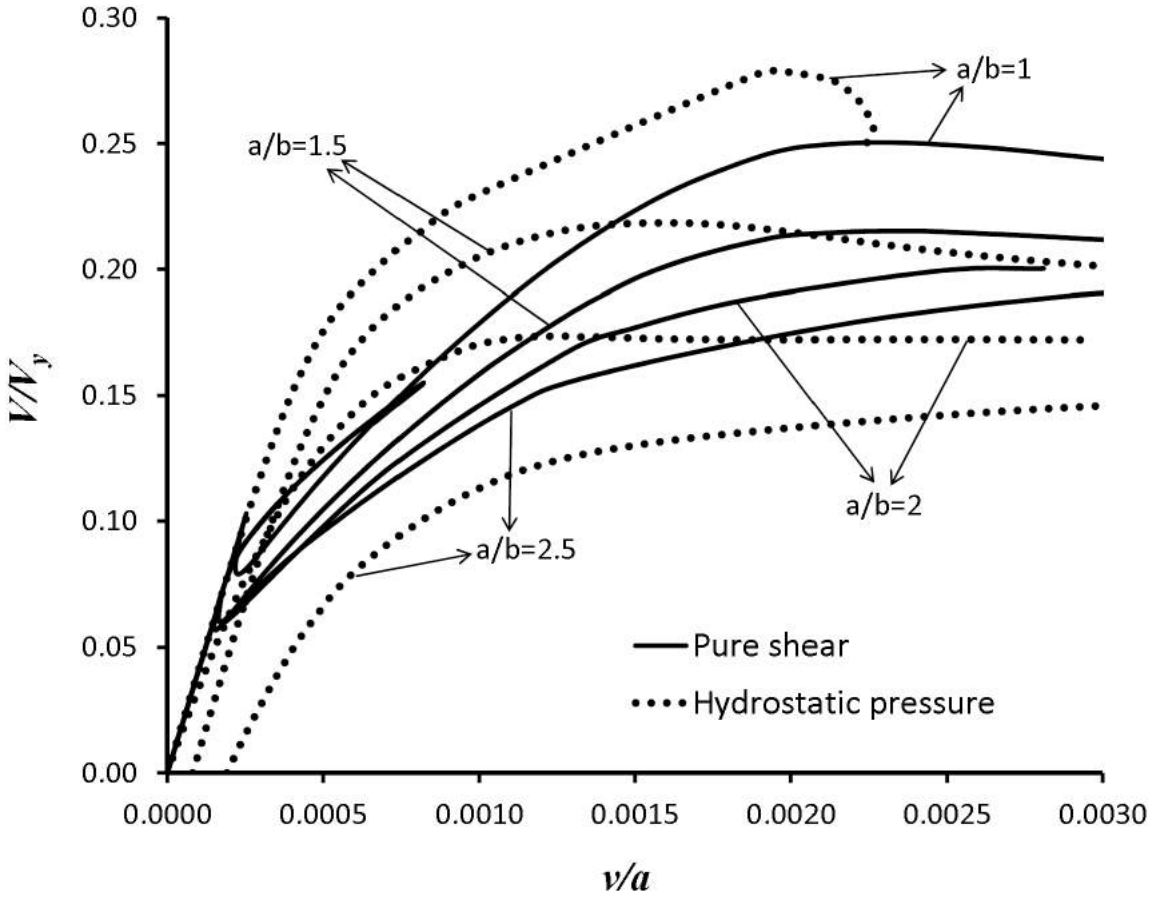

Fig. 24 Shear – circumferential displacement curves for panels with *Z=15* - Outward pressure

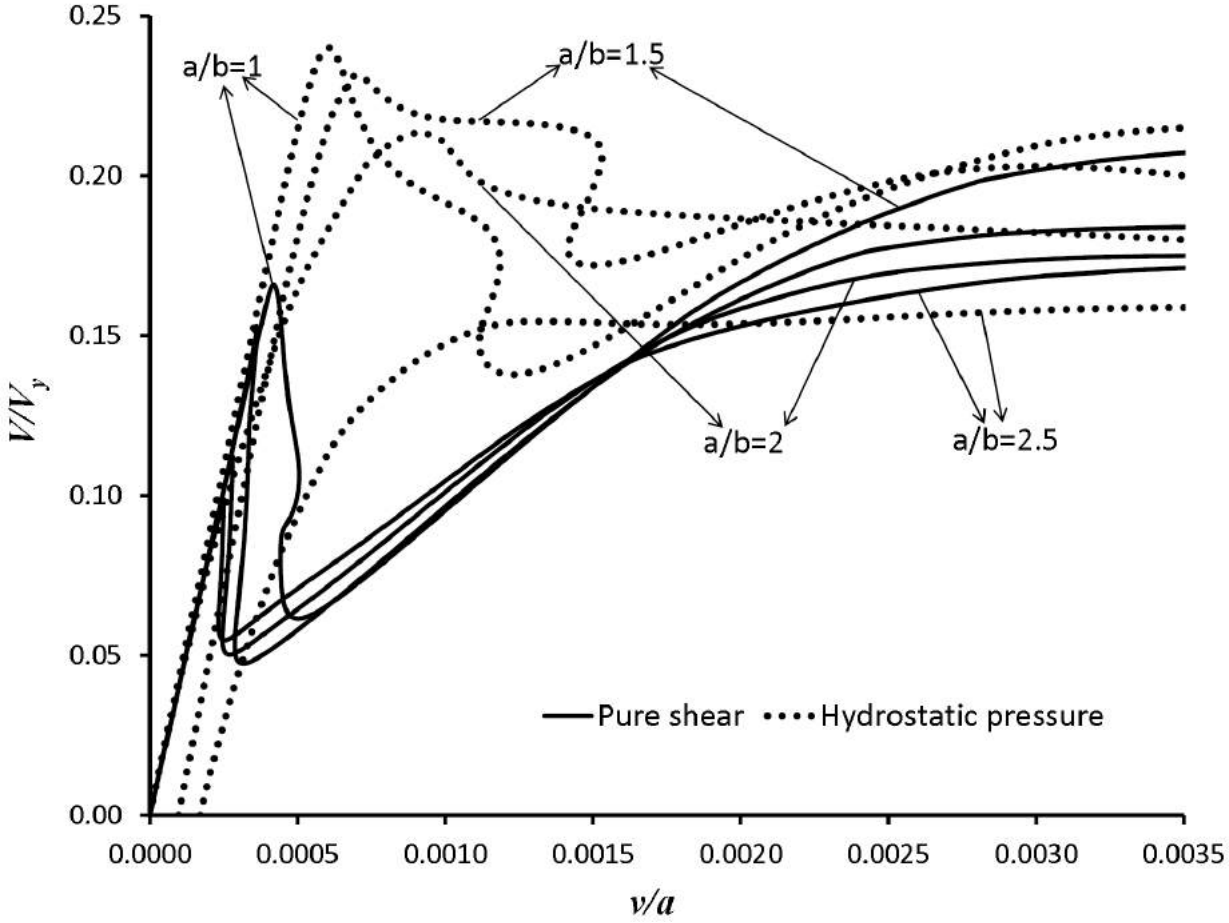

Fig. 25 Shear – circumferential displacement curves for panels with *Z=50* - Outward pressure

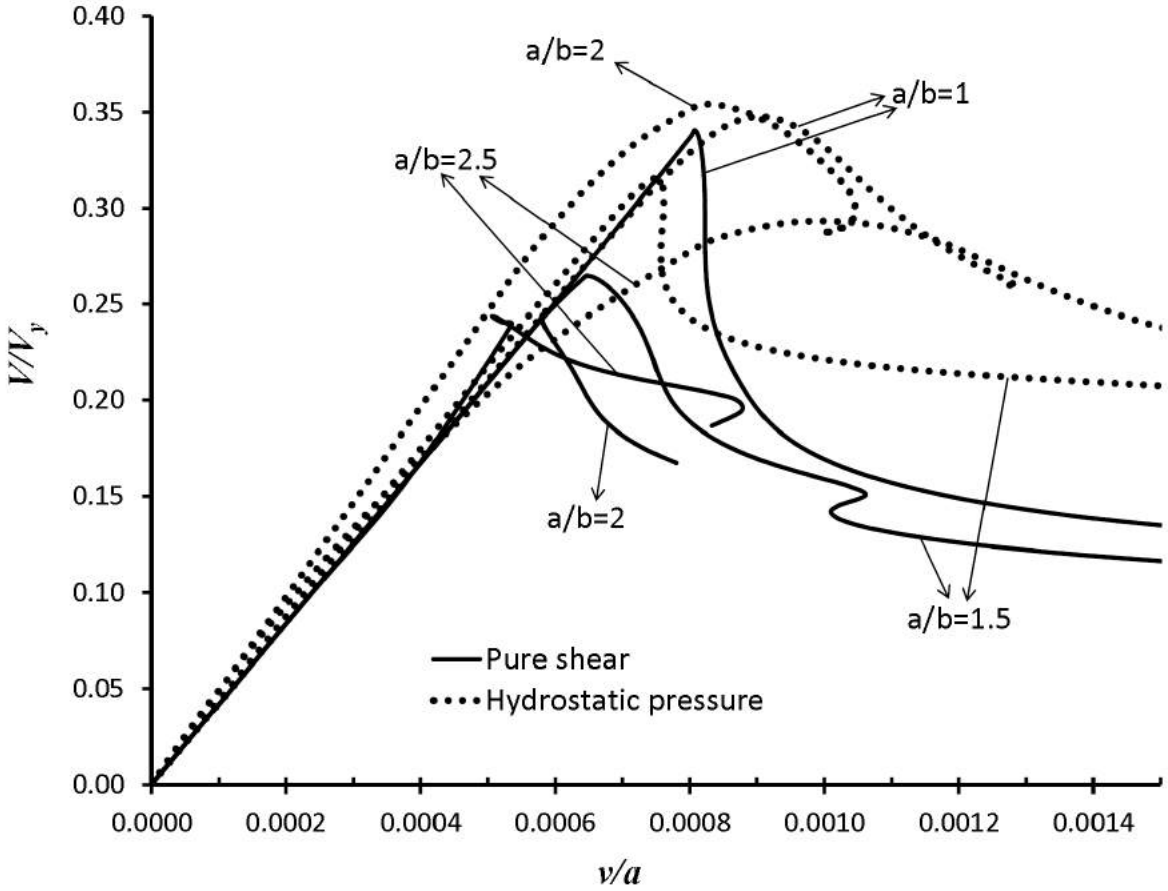

Fig. 26 Shear – circumferential displacement curves for panels with *Z=150* - Outward pressure

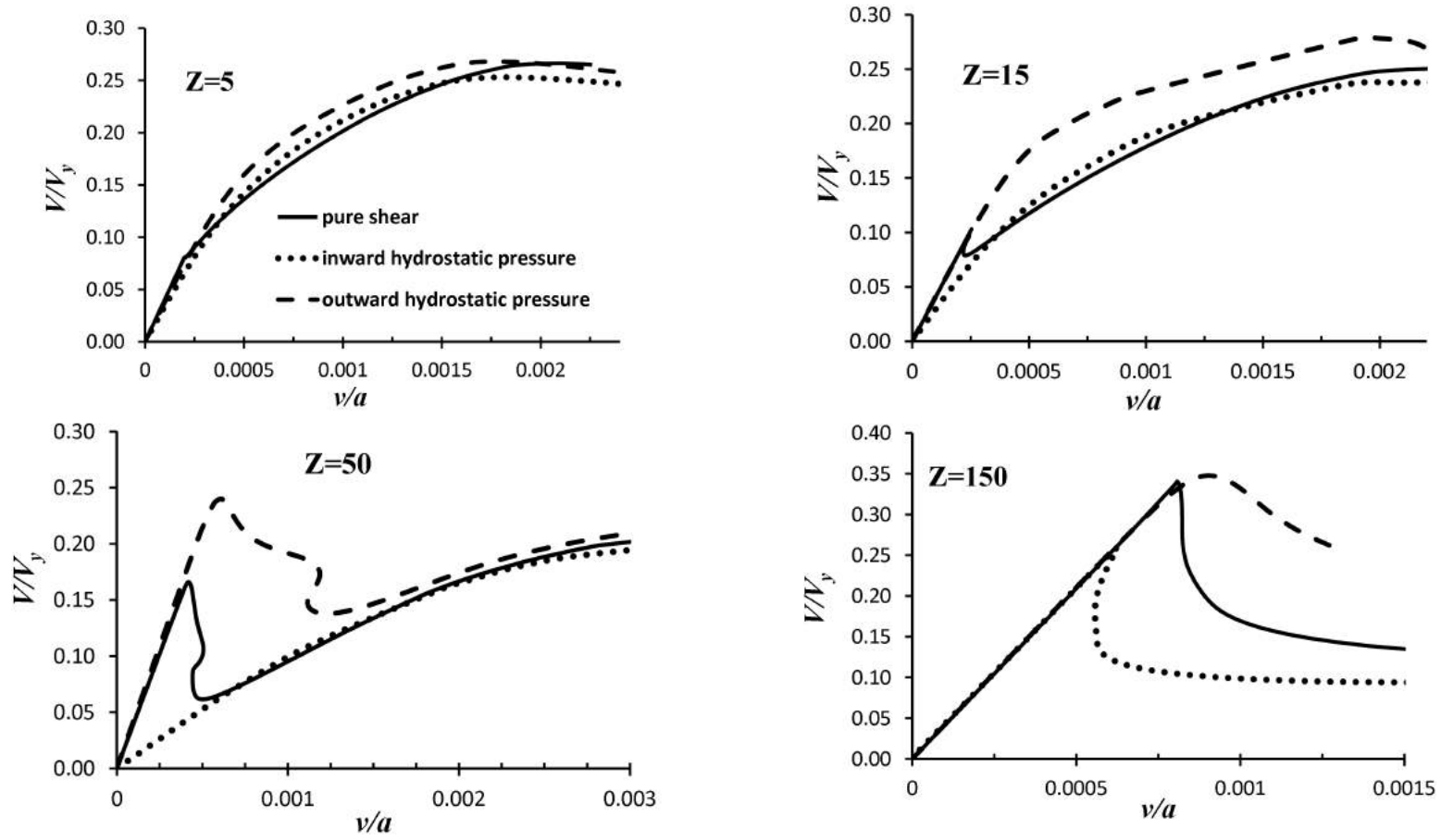

Fig. 27 **Comparison of effects of inward/outward hydrostatic pressures on the shear buckling behavior of various curvature square curved panels**

Table 1 Test Panel Dimensions

Specimen	*a=b*	*r*	*t*	*r/t*	*Z*
S1	18”(457mm)	44.8”(1138mm)	0.064”(1.62mm)	700	108
S2		64.0”(1626mm)		1000	75
S3		76.9”(1953mm)		1200	63

References

[1] M. Amani, B.L.O. Edlund, M.M. Alinia, Buckling and postbuckling behavior of unstiffened slender curved plates under uniform shear, Thin-Walled Structures 49(8) (2011) 1017-1031.
[2] L.H. Donnell, 'Stability of thin-walled tubes under torsion', NACA Report 479, 1933, National Advisory Committee for Aeronautics, Washington.
[3] W. Schneider, Y. Ribakov, Collapse analysis of thin walled cylindrical steel shells subjected to constant shear stress, Computers & structures 82(29) (2004) 2463-2470.
[4] D.M.A. Leggett, The Initial Buckling of Slightly Curved Panels Under Combined Shear and Compression. R. & M. No. 1972, British ARC 19(3) (1943).
[5] S.B. Batdorf, A simplified method of elastic-stability analysis for thin cylindrical shells, (1947).
[6] M.M. Domb, Nonlinear buckling predictions of curved panels under combined compression and shear loading, ICAS 2002 (2002).
[7] N. Rafal, Effect of normal pressure on the critical shear stress of curved sheet, DTIC Document, 1943.
[8] N. Rafel, C.W. Sandlin Jr, Effect of normal pressure on the critical compressive and shear stress of curved sheet, (1945).
[9] H.G. Hopkins, E.H. Brown, The effect of internal pressure on the initial buckling of thin-walled circular cylinders under torsion, HM Stationery Office1951.
[10] S. Aghajari, K. Abedi, H. Showkati, Buckling and post-buckling behavior of thin-walled cylindrical steel shells with varying thickness subjected to uniform external pressure, Thin-walled structures 44(8) (2006) 904-909.
[11] B.S. Golzan, H. Showkati, Buckling of thin-walled conical shells under uniform external pressure, Thin-Walled Structures 46(5) (2008) 516-529.
[12] L. Chen, J.M. Rotter, C. Doerich-Stavridis, Practical calculations for uniform external pressure buckling in cylindrical shells with stepped walls, Thin-Walled Structures 61 (2012) 162-168.
[13] E. Riks, The application of Newton's method to the problem of elastic stability, Journal of Applied Mechanics 39(4) (1972) 1060-1065.
[14] E. Riks, An incremental approach to the solution of snapping and buckling problems, International Journal of Solids and Structures 15(7) (1979) 529-551.
[15] T. Kobayashi, Y. Mihara, F. Fujii, Path-tracing analysis for post-buckling process of elastic cylindrical shells under axial compression, Thin-Walled Structures 61 (2012) 180-187.
[16] S. Wolfram, The MATHEMATICA® book, version 4, Cambridge university press1999.
[17] T.N. Chakherlou, A. Yaghoobi, Numerical simulation of residual stress relaxation around a cold-expanded fastener hole under longitudinal cyclic loading using different kinematic hardening models, Fatigue & Fracture of Engineering Materials & Structures 33(11) (2010) 740-751.
[18] A. Ghanbari, A. Rostami, M.M.S. Fakhrabadi, A. Yaghoobi, Simulation and analysis of anthropomorphic three finger micro/nano gripper using piezoelectric actuator, 2008.
[19] M. Ebad Sichani, M. Hanifehzadeh, J.E. Padgett, B. Gencturk, Probabilistic analysis of vertical concrete dry casks subjected to tip-over and aging effects, Nuclear Engineering and Design 343 (2019) 232-247.
[20] M. Ebad Sichani, J.E. Padgett, V. Bisadi, Probabilistic seismic analysis of concrete dry cask structures, Structural Safety 73 (2018) 87-98.
[21] A. Saeidpour, Fragility analysis of coastal bridges susceptible to hurricanes incorporating uncertainties in extreme wave parameters by means of wave spectra and enhancement of vulnerability assessment methodologies, Engineering, University of Georgia, 2017.
[22] A. Saeidpour, M. Amani, M.M. Alinia, Comparison of Postbuckling Prediction Approaches in Curved Panels, IABSE-IASS 2011 Symposium, London, UK, 2011.
[23] A. Saeidpour, M.G. Chorzepa, J. Christian, S. Durham, Parameterized Fragility Assessment of Bridges Subjected to Hurricane Events Using Metamodels and Multiple Environmental Parameters, Journal of Infrastructure Systems 24(4) (2018) 04018031.
[24] A. Saeidpour, M.G. Chorzepa, J. Christian, S. Durham, Probabilistic hurricane risk analysis of coastal bridges incorporating extreme wave statistics, Engineering Structures 182 (2019) 379-390.
[25] A. Users, Theory Manuals: Version 6.9-1, Abaqus Inc., USA (2009).
[26] H. Salehi, T. Taghikhany, Application of Robust-Optimum Algorithms in Semi-Active Control Strategy for Seismic Protection of Equipment, 15th World Conference on Earthquake Engineering, Portugal, 2012.
[27] H. Salehi, T. Taghikhany, A. Yeganeh Fallah, Seismic protection of vulnerable equipment with semi-active control by employing robust and clipped-optimal algorithms, International Journal of Civil Engineering 12(4) (2014) 413-428.
[28] A. Saeidpour, Analysis of Shear Buckling Behavior of Hydrostatic Pressured Curved Panels, Department of Civil Engineering, Amirkabir University of Technology (Tehran Polytechnic), 2011.
[29] A.A. Saeidpour, Mozhdeh; Alinia, Mohamad, Comparison of Postbuckling Prediction Approaches in Curved Panels, IABSE-IASS 2011 Symposium, London, 2011.

[30] B.L.O. Edlund, Buckling of metallic shells: Buckling and postbuckling behaviour of isotropic shells, especially cylinders, Structural Control and Health Monitoring 14(4) (2007) 693-713.